



MASTERARBEIT

Titel der Masterarbeit

The dimensions of the skeletal elements of the skulls of children from an historical collection from the 1830's and their use for the determination of age at death

verfasst von

Sandra Reithmayer BSc

angestrebter akademischer Grad

Master of Science (MSc)

Wien, 2015

Studienkennzahl lt. Studienblatt: A 066 827
Studienrichtung lt. Studienblatt: Masterstudium Anthropologie
Betreut von: a.o. Univ.-Prof. MMag. Dr. Sylvia Kirchengast

Table of Contents

ACKNOWLEDGEMENTS.....	5
ABSTRACT	6
ZUSAMMENFASSUNG.....	7
1 INTRODUCTION	9
2 THEORETICAL PRINCIPLES.....	10
2.1 Forensic osteology and age estimation	10
2.2 Forensic fetal osteology and fetal age estimation.....	11
2.3 Age estimation based on the skull	12
2.3.1 Anatomical characteristics of the human skull.....	13
Viscerocranium and neurocranium	14
Fontanelles	14
Sutures	16
2.3.2 The intrauterine development of the human skull	17
Chondrocranium	17
Desmocranium	17
Viscerocranium	18
2.3.3 Studies of age estimation in infant skulls	18
2.4 The current study: six fetal skull bones for age estimation.....	19
2.4.1 The occipital bone.....	20
2.4.2 The parietal bone	22
2.4.3 The frontal bone.....	23
2.4.4 The zygomatic bone	24
2.4.5 The maxilla.....	25
2.4.6 The mandible.....	26
3 OBJECTIVES	27

4	MATERIALS AND METHODS	28
4.1	Material	28
4.2	Methods	34
4.2.1	Description of the measurements of all analysed skull bones	34
4.2.2	Statistical analysis	43
5	RESULTS	44
5.1	Descriptive statistics	44
5.2	Regression models	46
5.2.1	The chord height of the pars squama occipitalis	46
5.2.2	The chord width of the pars squama occipitalis	47
5.2.3	The maximum width of the pars basilaris occipitalis	48
5.2.4	The sagittal length of the pars basilaris occipitalis	49
5.2.5	The maximum length of the pars basilaris occipitalis	50
5.2.6	Comparison of the length of the pars basilaris vs. the width of the pars basilaris	51
5.2.7	The chord height of the parietal bone	52
5.2.8	The chord width of the parietal bone	53
5.2.9	The chord height of the frontal bone	54
5.2.10	The chord width of the frontal bone	55
5.2.11	The length of the zygomatic bone	56
5.2.12	The oblique height (width) of the zygomatic bone	57
5.2.13	The length of the maxilla	58
5.2.14	The body length of the mandible	59
5.2.15	The width of the mandible	60
5.2.16	The oblique length of the mandible	61
6	DISCUSSION	63
6.1	The most and least suitable measurements of this study	64
6.1.1	Measurements best suited for the estimation of age at death	64
6.1.2	Measurements least suited for the estimation of age at death	64
6.1.3	The regression equations	65
6.2	Factors influencing the reliability of age estimation	65
6.3	Interpretation of the results of this study in comparison to previously published data ...	66
6.3.1	Mandible	66

6.3.2	Frontal bone, zygomatic bone, maxilla and pars squama occipitalis	67
6.3.3	Pars basilaris occipitalis.....	67
6.4	Conclusion and outlook	69
	REFERENCES	70
	LIST OF FIGURES	75
	LIST OF TABLES	77
	ABBREVIATIONS	78
	SUPPLEMENTAL MATERIAL	79
	CURRICULUM VITAE	82

Acknowledgements

I want to thank Univ.-Prof. Dr. Sylvia Kirchengast from the Department of Anthropology of the University of Vienna for being my thesis supervisor.

Special thanks to Mag. Stefan Tangl from the Karl Donath Laboratory for Hard Tissue and Biomaterial Research, Vienna, for his support and valuable suggestions. His guidance was quite helpful during all the time of research and writing this thesis.

I want to express my gratitude to Sonja Kuderer for her valuable review and giving me special points of attention for my master thesis.

Many thanks to Stefan Lettner, who gave me support for my data analysis. I also want to thank Toni Dobsak and Patrick Heimel, who helped me when working with the computer.

My sincere thanks also go to Dr. Gabriele Dorffner from the „Zahnmuseum Wien“ for her time and her special advice regarding the Terzer collection.

At this point, I would like to thank my friends who supported me, especially Margherita Fink and Judith Hagenhofer for encouraging me.

Finally, I want to thank my father who always supported me and believed in me. I would like to thank him for all he has done for me. Without him I would not have come this far!

Abstract

The estimation of the age at death of fetal and juvenile skeletons is a fundamental topic in forensic anthropology and bioarchaeological studies. Especially the examination of individual skull bones can provide a large information yield for determining the age at death.

For the present study 32 skulls of children with a known age between seven months in utero and two and 2.5 years have been examined. The historical sample from the 1830's originates from the Viennese Foundling House and was collected by Valentin Terzer, a surgeon, dentist and obstetrician. The dimensions of six different skull bones (occipital, parietal, frontal, zygomatic, maxilla and mandible) of these infants were measured with a sliding caliper. By using linear and quadratic regression equations, the association between these skull dimensions and the juvenile age at death could be described.

The statistical evaluation revealed that the coefficients of determination R^2 of all skull measurements ranged between 0.38 and 0.83. The most accurate method to determine the age at death of children by means of regression equations was the measurement of the frontal bone chord height. The least reliable estimates were obtained when using the width of the mandible. Although a good validity of pars basilaris occipitalis measurements for ageing of sub-adults was asserted in earlier research, these assumptions could not be confirmed by the data of this study. Additionally, the maximum width, sagittal length and maximum length of the pars basilaris occipitalis had only a poor predictive value for the infant's age in this project.

The results of this osteological study indicate that linear and quadratic regression equations can be meaningfully applied for the estimation of age at death using skull bone measurements. Hence, this should encourage additional scientific work in this field, which examines the relation between skull bone measurements and age at death of infants. Thereby future research should concentrate on developing valid and reproducible standards for ageing methods based on skull measurements since these methods can be used in numerous bioarchaeological and forensic contexts.

Zusammenfassung

Die Bestimmung des Sterbealters von fetalen und frühkindlichen Skeletten ist eine grundlegende Fragestellung der forensischen Anthropologie wie auch in der Durchführung bioarchäologischer Studien. Insbesondere die Untersuchung einzelner Schädelknochen kann zahlreiche Informationen für die Bestimmung des Sterbealters liefern.

Für die vorliegende Studie wurden 32 Schädel von Kindern mit einem bekannten Sterbealter zwischen sieben Monaten in utero und zweieinhalb Jahren untersucht. Die historische Sammlung aus den 1830er Jahren stammt aus einem Wiener Findelhaus und wurde von Valentin Terzer, einem Chirurgen, Zahnarzt und Geburtshelfer, gesammelt. Die Dimensionen von sechs verschiedenen Schädelknochen (Occipitale, Parietale, Frontale, Zygomaticum, Maxilla und Mandibel) dieser Kinder wurde mit einem Gleitzirkel gemessen. Durch die Verwendung von linearen und quadratischen Regressionsgleichungen konnte der Zusammenhang zwischen diesen Schädelmessungen und dem Sterbealter der Kinder beschrieben werden.

Die statistische Auswertung zeigt, dass der Bestimmungskoeffizient R^2 aller Schädelmessungen zwischen 0,38 und 0,83 variierte. Die genaueste Methode, um das Sterbealter von Kindern unter Verwendung von Regressionsgleichungen festzustellen, war die Messung der Höhe des Os frontale. Die am wenigsten zuverlässigen Schätzungen wurden bei Verwendung der Breite der Mandibula erzielt. Obwohl der Messungen der Pars basilaris occipitalis in früheren Untersuchungen eine hohe Aussagekraft für die Bestimmung des Sterbealters von Kindern zugeschrieben wurde, konnte dies durch die Daten dieser Studie nicht bestätigt werden. Außerdem hatten in der vorliegenden Arbeit die Messungen der maximalen Breite, der sagittalen Länge und der maximalen Länge der Pars basilaris occipitalis eine nur geringe Aussagekraft für die Schätzung des Sterbealters der Kinder.

Die Ergebnisse dieser osteologischen Studie zeigen, dass mittels linearer und quadratischer Regressionsgleichungen, die auf Schädelmaßen basieren, aussagekräftige Schätzungen des Sterbealters erzielt werden können.

Dies sollte daher zu weiteren wissenschaftlichen Arbeiten ermutigen, welche die Beziehung zwischen Messungen von Schädelknochen und der Bestimmung des Sterbealters von Kindern untersuchen. Daher sollte sich die zukünftige Forschungsarbeit auf die Entwicklung aussagekräftiger und reproduzierbarer Standards für die Bestimmung des Sterbealters durch Schädelmessungen konzentrieren, da diese Methoden in zahlreichen bioarchäologischen und forensischen Fragestellungen verwendet werden können.

1 Introduction

Fetal and juvenile osteology are important fields within forensic anthropology and medico-legal medicine. (1) Such research areas benefit from examinations of sub-adult skeletons as these can provide a lot of information (2) on the general health, the wellbeing of a population as well as on mortality and birth rates. An important first step in this regard is the estimation of individual age of skeletal remains. Fetal and new-born age estimation rely mainly on dentition-based methods (3), on the measurement of long bones (4) as well as on the examination of ossification centres. (5)

A rather rare approach to age sub-adults is the analysis and survey of individual skull bones. Up to now there exist only few studies, which described a relation between the chronological age of an individual and the dimensions of the occipital bone (5) (6) (7) (8) (9) (10) (11) and the mandible (12) (13) (14). Other bony parts of the skull were widely neglected in age estimation research so far.

This study therefore investigates the correlation between the measurements of six skull bones (occipital, parietal, frontal, zygomatic, maxilla and mandible) and sub-adult age. These numerous measurements were taken with a sliding caliper on 32 skulls of the so-called Terzer collection, a group of infants from the Viennese Foundling House which were compiled in the 1830's. The known age at death of these children lay between seven months in utero and two years, seven months and 22 days. By applying linear and quadratic models, a reliable statistical method was used to calculate regression equations, which characterize the association between age-at-death and skull dimensions in infants and allow to calculate an estimated age of the individual.

2 Theoretical principles

2.1 Forensic osteology and age estimation

In the field of forensic osteology skeletal remains are analysed. Thereby the skeletal dimensions, anthropological characteristics as well as the physical development of skeletons are investigated. Additionally, this scientific area determines the origin and age of discovered human remains. (5)

The aim of such an analysis is the identification of individuals by examining four main characteristics - sex, age, stature and ethnic background. (15) Age estimation is the first step for further investigations in forensic and archaeological cases. A determination of the individual's age is of particular importance as this information is essential for a positive identification. (2)

Skeletal development and bone growth, which are crucial for estimating the age of skeletal remains, however depend on various external factors. (15) These can have a genetic, environmental, nutritional and socioeconomic basis (2) and possibly complicate age estimation analyses by raising individual variation in skeletal appearance within and between populations.

The changes of morphological characteristics in dentition and skeletal growth during the various stages of life are generally utilized to determine age. The age of remains is assessed on a skeletal basis by the presence or absence of ossification centres as well as from the size and length of long bones. (5) (15) (16) (17) (18) Moreover, dental age identification is possible when comparing the eruption and the degree of mineralization of individuals. (15) (19) (20) (21) For comparative purposes there are up to now many standards for dentition development and changes available in the literature. (22) (23) (24) (25)

2.2 Forensic fetal osteology and fetal age estimation

Fetal osteology is a special branch of forensic osteology which is concentrating on the examination of fetal skeletons. (5) When a skeleton of a fetus is found, the following questions have to be answered by medico-legal experts at the beginning: (5)

1. Are the remains of human fetal or of animal origin?
2. If the bones stem from a human fetus, what is the lunar age?
3. Could the fetus have been viable at birth, or was it born prematurely, in a non-viable state?
4. Is there serological or genetic evidence that the fetus is related to possible suspects?
5. Did the investigation or skeleton itself furnish data indicating the circumstances or the possible cause of death?
6. How much time has elapsed between the interment of the fetus and its discovery?

It is not always an easy task to work with, recognize and analyse fetal remains. (5) (2) Firstly, fetal bones might be easily overlooked or misinterpreted during osteological work due to inadequate excavation techniques. In addition, skeletons of sub-adults and particularly those from fetuses and infants can be confused with animal bone. Moreover, the fragility of fetal remains as well as their smaller size and density than those of adults makes these bones more susceptible to decay, loss or dispersion. (2) (26) The manifold stages of development, the large number of skeletal elements present as well as their varying appearance might further impede skeletal investigations. (2)

Despite some constraints in the handling of fetal bones, a biological identification and the age determination of juveniles can be a useful source of information as these factors reflect the general health and wellbeing of a population. (27) Moreover, sub-adult skeletal remains give insights into population size and structure as well as into mortality and birth rates. (2)

When a complete fetal skeleton is recovered, questions of its age at death, the lunar month and its maturity at birth can be answered by a comparison with generally accepted osteometrical data and standards. (1) (5) This can be achieved as the increase of osteological dimensions with growth and the succession of well documented developmental changes allow a reliable age estimation. (15) (24) (28) Therefore, fetal and new-born age estimation is concentrating on methods that utilize changes in child development and enable thereby the assignment of a developmental stage. These include analyses of changes in the dentition (29) (3) and of the presence or absence of ossification centres. (5) (30) Fetuses can further be aged according to their long bone development (4) by measuring diaphyseal length of e.g. the tibia or humerus. (4) The standard method for fetal age determination is the measurement of the femoral diaphysis, which is based on the various empirical charts and regression formulas. (14) (27) (31) Dental development is claimed to be the most accurate method to determine the age in immature skeletons. (32)

Also more unusual approaches of estimating the infant's age can be found in the literature. Hence, a relation between fetal clavicular measurements and the age was already demonstrated. (33) Some studies introduced correlations between the age of new-borns or fetuses and morphometric indices of the cervical vertebral column. (34) (35) (36) (37) Even facial dimensions were related to fetal age. (38) (39) In particular an association between mandibular distances and the fetal age were found in previously published research. (12) (13) (14) As this thesis relies on the measurement of bony skull elements, the next chapter will give a short introduction into skull-based age estimation in young infants.

2.3 Age estimation based on the skull

The human origin as well as the age at death of a recovered specimen can be determined by examining the skull bones. One advantage when working with skull bones is their good representation and preservation in the burial environment. (40) Especially cranial bones such as the temporal, the occipital, the zygomatic and the mandible are well preserved and often found completely intact and therefore allow the age determination of skeletons. (40)

According to Scheuer and Black, for example the measurement of the pars basilaris of the occipital is an attractive tool for age estimations as the proportions of the pars basilaris change within life and the bone remains intact after burial. (27)

An easy method to relate the skull to age was proposed by Sherwood et al. (2000), who revealed a relation between the head circumference and age in fetuses between 15 and 42 weeks of gestational age. (17) In addition, the individual maturation, morphological changes and developmental stages of the skull provide the basis for a good and simple estimation of age at death in sub-adults. Since the skull is one of those main skeletal elements where a joining of primary ossification centres occurs, a knowledge of the timing and schedule of these watershed events can be used for age determination in sub-adults. (41) Cranial maturation – the closure of fontanelles or suture formation – has already been applied as the aging method of choice in infants in previous studies. (42) (43) The next chapters provide a short overview about the most important anatomical characteristics of the human and in particular the sub-adult skull.

2.3.1 Anatomical characteristics of the human skull

The skull or cranium is the most complex region of the axial skeleton and contains 28 bones, which form the cranial vault, the face and the jaws. (2) These bones support and protect the brain and sensory organs. Moreover, the human skull also contains the upper parts of the respiratory and alimentary tracts. (4)

At birth the skull consists of 45 separate elements. (44) These further ossify from multiple ossification centres and result in a final number of 28 bones in an adult cranium. (2) A skull of a new-born is relatively large compared to other parts of the body (44) and shows different proportions compared to those of adults. (4) (27) To be more precise, the new-born skull has a very small facial cranium whereas the vault is commensurably oversized. (44)

Whilst almost all parts of the face develop in parallel with the formation of the dentition, the vault and the eye-sockets are growing more rapidly. (4) (27) The fetal face at birth corresponds to 55 - 60% of the breadth, 40 - 45% of the height and 30 - 35 % of the depth of an adult face. (45) Additionally, the rate of calvarial to facial proportions changes from about 8:1 at birth, to 4:1 at five years and to 2 - 2.5: 1 in adult life. (46)

Viscerocranium and neurocranium

The cranium consists of two parts: the neurocranium and the viscerocranium. (4) (47) The neurocranium, the braincase, is constituted of eight bones (the ethmoid, the frontal, the occipital, two parietals, the sphenoid and two temporals). It contains a base and a vault whose sidewalls and roof (calvaria) complete the bony protective covering. The viscerocranium comprises 14 facial bones (two inferior nasal conchae, two lacrimal bones, the mandible, two maxillae, two nasal bones, two palatine bones, the vomer and two zygomatic bones) yielding an upper part, which forms the skeleton of the orbits as well as of the nose, and a lower part that consisting of the maxilla and mandibular bone. (4) (47)

Fontanelles

At birth the skull reveals “soft spots” between the cranial plates, the so-called fontanelles, which are formed by connective tissue. Fontanelles are cartilaginous membranes that mineralize and turn to bone during life. (44)

The anterior or bregmatic fontanelle lies between the two parietals and the two halves of the frontal and is four-sided (Figure 1). It closes at the age of three years. (48) (49) An analysis of the anterior fontanelle is important after birth (48) as it can be used for taking a blood sample or giving intravenous injections. (49)

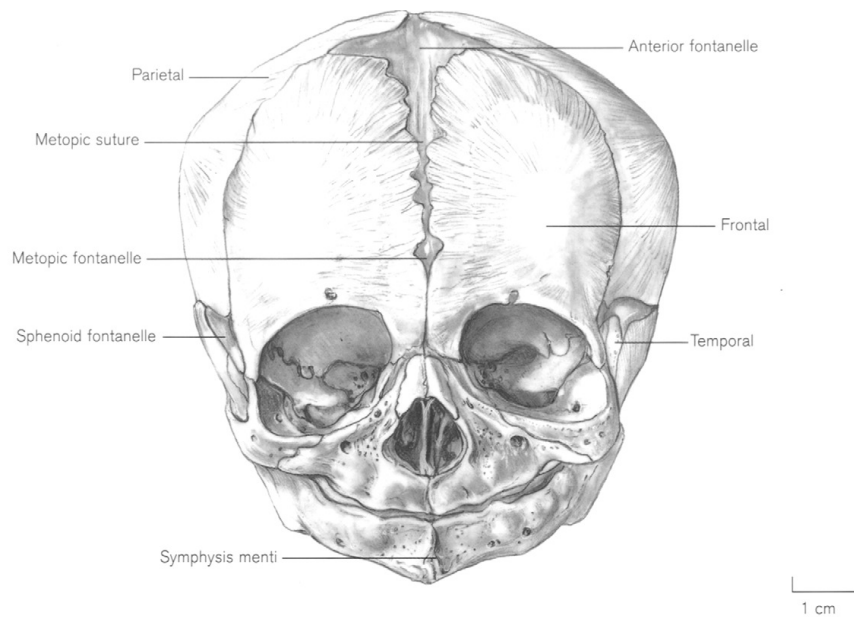


Figure 1: Anterior view of the fetal skull. (4)

The posterior or lambdoid fontanelle is triangular and located between the occipital and parietals (Figure 2 and Figure 3). It closes in the third month of postnatal life. (48) (49)

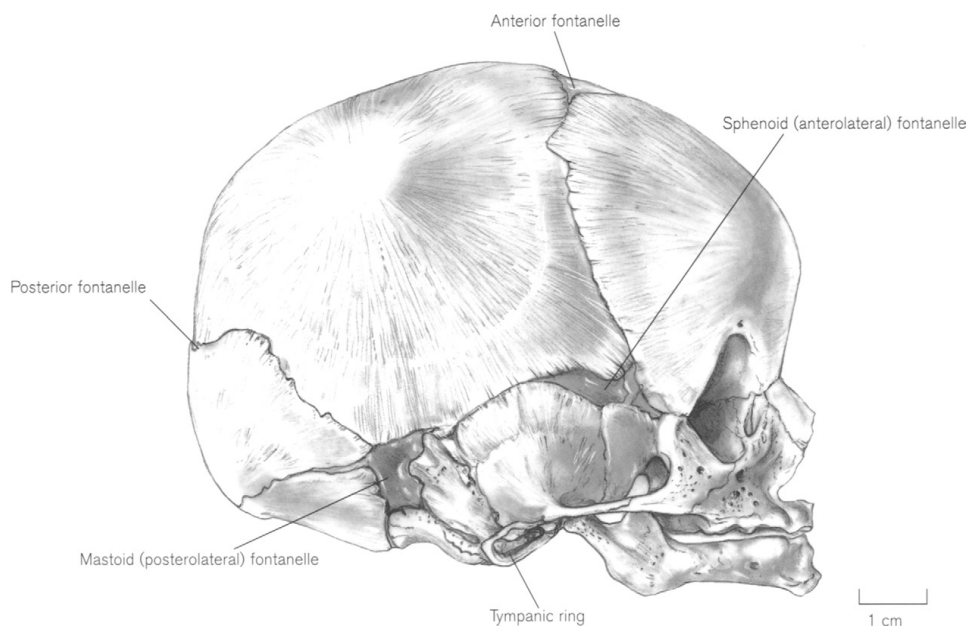


Figure 2: Lateral view of the fetal skull. (4)

The two types of laterally located fontanelles are called sphenoid and mastoid fontanelle. The sphenoid or anterolateral fontanelles lie between the frontal, parietal, temporal and sphenoid (Figure 2) and close by the sixth month of life. The mastoid or posterolateral fontanelle, which is placed between the temporal, parietal and occipital, closes in the 18th month of life (Figure 2 and Figure 3). (49)

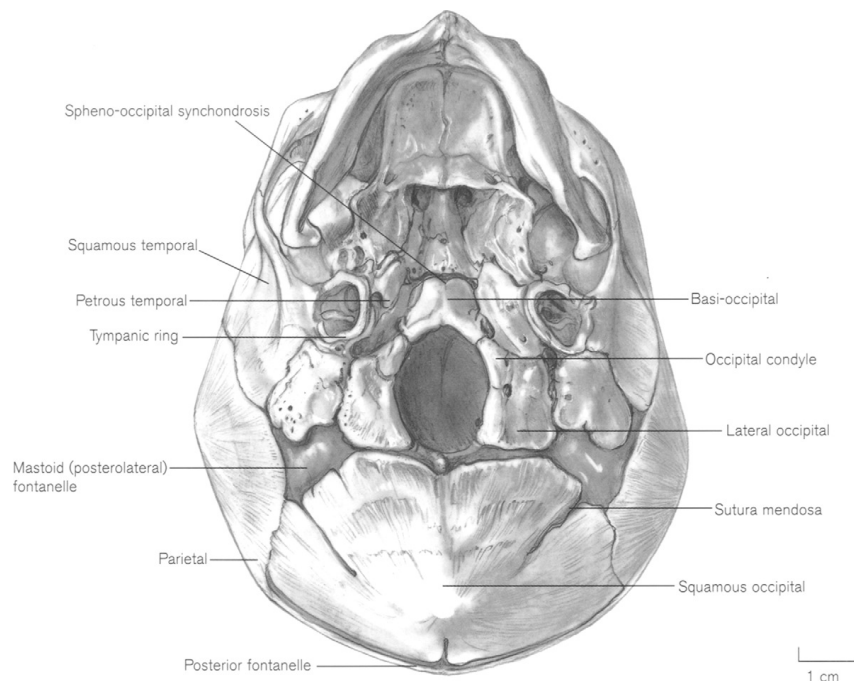


Figure 3: Basal view of the fetal skull. (4)

Sutures

Sutures are the contact lines between skull bones, which have a zipper-like appearance. The names of many sutures derive from the two bones contacting each other. (44) The numerous bones of the vault come into complete contact at the age of four or five years (48).

2.3.2 The intrauterine development of the human skull

The prenatal development of the human skull is complex, as it is a mosaic of a number of distinct components. (46) The developmental processes include changes in morphology and growth of the three main parts, the desmocranium, the chondrocranium and the viscerocranium. (46) The neurocranium is formed from the desmo- and the chondrocranium whereas the viscerocranium develops into the face. (46)

Chondrocranium

The initially formed, cartilaginous part of the skull is called chondrocranium. The development of the chondrocranium starts at the end of the fourth intrauterine week and is finished in the ninth week at the latest. It is formed from endochondral bone of neural crest origin. (46) When the chondrocranium is ossified, starting from different ossification centres, it forms the essential part of the base of skull. (49) This transformation of the chondrocranium into the cranial base starts in parallel with the ossification of the membranous roof of the skull. Only the nasal septum and the greater wings of the sphenoid persist in a cartilaginous condition. (5) The occipital bone (except for the superior portion of the squama), the ethmoid bone, the sphenoid bone (except for the pterygoid plates and tip of the greater wing), the temporal bone (except for the superior portion of the squama and the tympanic part) and the inferior concha develop from the chondrocranium. (5)

Desmocranium

The mesenchymic part of the skull, the desmocranium, is formed from intramembranous bone of paraxial mesodermal origin. (46) The desmocranium forms the vault of the skull (the calvaria) after its ossification and it builds the major part of the bones of the viscerocranium. (49) The parietal bone, the frontal bone, the nasal bone, the lacrimal bone, the vomer and the upper part of the squama occipitalis arise from the desmocranium at the beginning of the third month. (5)

Viscerocranium

The viscerocranium forms the facial skull and is derived from the pharyngeal arches. (46) A large number of the bones of the viscerocranium is built by the desmocranium. (49) The viscerocranium forms the access to the visual, aural and respiratory system as well as the oromasticatory apparatus. (46)

2.3.3 Studies of age estimation in infant skulls

With regard to age estimation, there appears to be less literature present on the measurements of infant skulls than on the rest of the skeleton or the teeth. (50) Not only skull circumferences but also dimensions of individual skull bones might be of importance for age analyses but these still have to be studied in detail. (51) Some previous studies could already reveal how separate bones of the skull can be used for the age estimation of fetuses and juveniles.

Fazekas & Kósa (1978) measured all bones of the skeleton of male and female fetuses from the third to the tenth lunar month of pregnancy. (5) They measured the length and width of the basilar part and developed standards for a fetal age estimation based on the pars basilaris. (5)

Redfield (1970) examined the occipital bone of 117 skeletons from the medieval necropolis at Mistihalj, in Southern Yugoslavia. (6) All measurements of the occipital bone were regular enough to allow a prediction of age. The sample was further compared with a series of 20 German fetuses, ten Egyptian skulls and 19 Eskimo skeletons. Thereby Redfield found, that the data could also be used for approximating age of skeletons in the fetal and early post-natal range in other populations. (6)

The work by Scheuer and MacLaughlin-Black (1994) confirmed a correlation between the age at death and the dimensions of the pars basilaris of the occipital bone in fetuses and juveniles. (7) They studied 62 fetal and juvenile partes basillares of the St. Bride's and Spitalfields collection, ranging in the age from approximately 26 weeks in utero to four years and seven months postpartum.

Further, Scheuer and MacLauglin-Black increased the number of measurements and additionally also studied the proportion of the maximum width to the sagittal length (5) as well as the maximum length of the pars basilaris in regard to their validity as age indicators. (6)

Tocheri & Molto (2005) analysed 39 fetal and juvenile skeletons from Kellis 2 (K2), a Roman Period cemetery in Dakhleh, Egypt including the measurement of the basilar part. (8) They found that the dimensions of the basilar part were related to the gestational age. Unfortunately the real chronological age of the specimens was not known, but only estimated using femoral diaphyseal length and dental data. (8)

In their studies Nagaoka et al. (2012) provided more data on the relation between the fetal age at death and the basilar part of the occipital bone. (10) (9) By investigating 272 Japanese individuals between the ages of five to eleven months from gestation they discovered that the fetal age at death can be directly inferred from basilar part measurements. (10) (9) In addition, a positive correlation between the measurements of the temporal bones with gestational age could be revealed by Nagaoka et al. (2012). The petrous part of the temporal was a good marker for the estimation of age at death in their Japanese sample. (10) (9)

The investigation by Cardoso et al. (2013) introduces the possible utility of ossification centres in the occipital bone as markers for age estimation. (11) In a sample of 64 immature skeletons between birth and eight years of age they could demonstrate the relation between age and a certain stage of fusion. (11)

2.4 The current study: six fetal skull bones for age estimation

Following Fazekas and Kòsa (1978), Redfield (1970), Scheuer and MacLauglin-Black (1994) and others, in this thesis six different bones from sub-adult skulls were measured and used for an age determination. (5–7) The characteristics and the development of each bone analysed will be shortly described below.

2.4.1 The occipital bone

The occipital bone forms the base of the skull and surrounds the foramen magnum on each side. It comprises the squama occipitalis, two partes laterales os occipitalis and the pars basilaris os occipitalis. All four parts are present long before birth and fuse from posterior to anterior in the first six years of life. (6)

The base of the skull is the “most stable area in the skull during growth”, which is normally not distorted during the birth process. (52) Especially the pars basilaris is a complete and solid bone from an early fetal period on, which is likely to be found unbroken. (6) In addition, all the bones of the base are highly resistant to degradation and have characteristic shapes (Figure 4). Hence, for skeletal research the bones of the base are usually found in an intact condition and have characteristic features useful for identification, which is important for age at death determinations. (5)

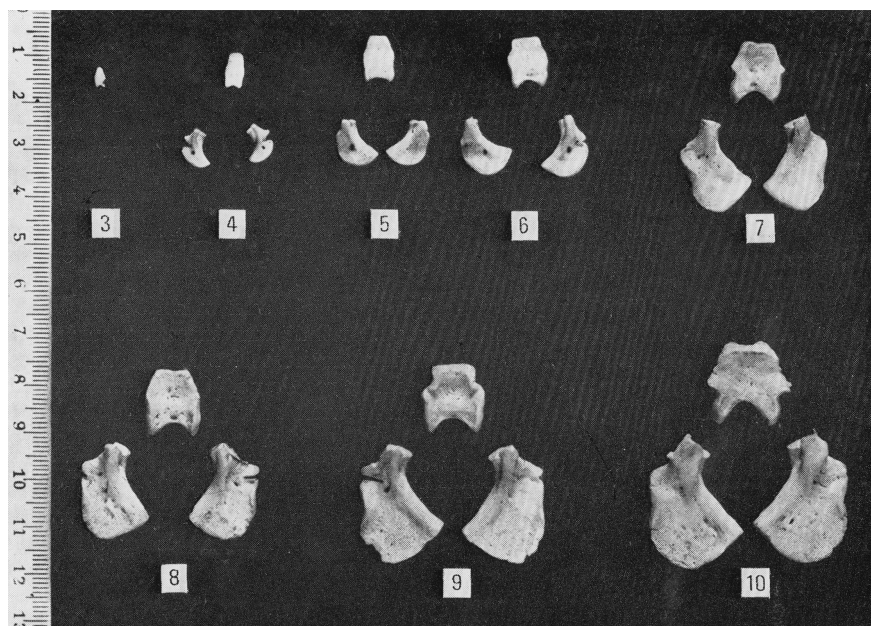


Figure 4: Basilar and lateral parts of the occipital bone at the age of 3 - 10 lunar months. (5)

The **pars basilaris os occipitalis** is centred under the skull and located anterior to the foramen magnum. It forms the base of the skull and is separated from the sphenoid bone by the synchondrosis spheno-occipitalis. (6) The pars basilaris os occipitalis experiences characteristic changes during the intrauterine development.(5)

Thereby it gradually thickens and increases in width. From the age of 8 ½ lunar months, the width of the bone usually starts to exceed its length (Figure 4). (5) By six months of age is the width of the pars basilaris always greater than its length. (27)

The **squama occipitalis** consists of the pars supra-occipitalis, the most posterior part of the skull base, and the pars interparietalis. It forms the posterior section of the occipital bone. (27) The pars supra-occipitalis and the pars interparietalis start to fuse in the middle of the bone between 3.5 and 5 prenatal months. (6) The junction of these two bones is marked by the sutura mendosa in prenatal life (Figure 5). (27) During the first year of life the remains of the sutura mendosa are closing. (27)

The two **pars lateralis os occipitalis** lie on either side of the foramen magnum and articulate anteriorly with the pars basilaris os occipitalis. (6) (27) The anterior ends of either pars lateralis thicken gradually and in this region does the hypoglossal canal pass through (Figure 5). (27) (5)

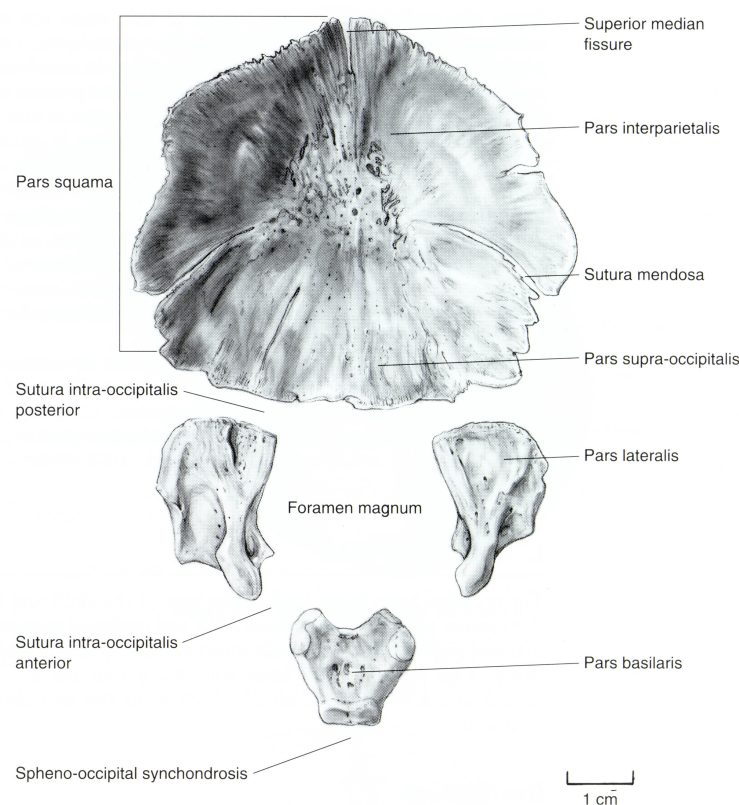


Figure 5: Intracranial view of the perinatal occipital bone. (27)

2.4.2 The parietal bone

The parietal bone is a paired bone, which forms a large part of the sidewalls of the cranial cavity. At the sagittal suture both parietal bones articulate with each other and other sutures with the squama occipitalis, the mastoid, the squamous part of the temporal, the greater wings of the sphenoid and the frontal. (27)

At the end of the second lunar month two ossification centres develop. In the fifth lunar month the squamous plate in the region of the parietal eminence grows in density and is ellipsoid as well as convex in shape. (5) The margins of the squamous part straighten at the coronal, sagittal and lambdoid sutures in the sixth lunar month. Then both superior ends become angular (5) and borders as well as angles become definitive. (27) At birth there exists a single parietal bone with a prominent eminence (Figure 6) and the sagittal fontanelle is usually no longer present. (27)

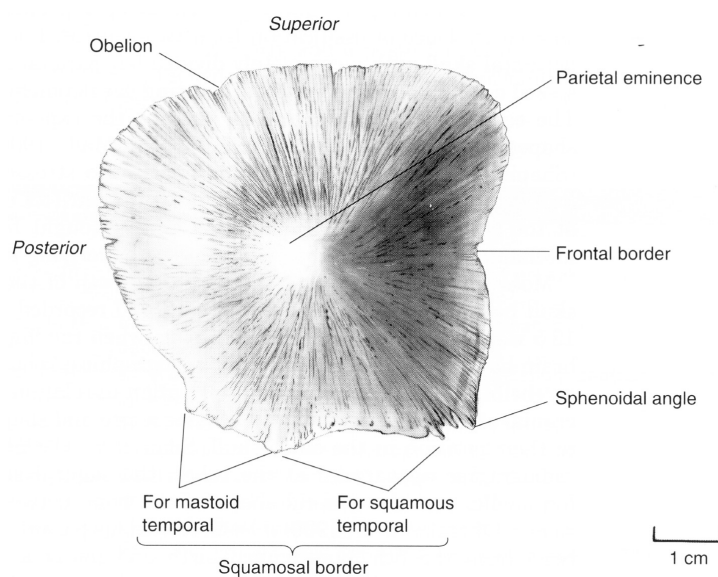


Figure 6: The right perinatal parietal bone. (27)

2.4.3 The frontal bone

The frontal bone is an irregular and bowl-shaped bone, which forms parts of the roof and the sidewalls of the cranial cavity. It also builds the floor of the anterior cranial fossa and of the roofs of the orbits. (27) The bone consists of two independent symmetrical parts and is divided by the frontal suture. (5)

Between six and seven weeks of prenatal life, each half of the bone ossifies from a single centre. (27) If no complete union of both frontal bones takes place, the bones meet by the sutura metopica (in 10 % of cases). (5) At the end of the first trimester a merged frontal bone is recognizable. It is built of two symmetrical halves at birth, which are separated from each other by the metopic suture. (27) In the fifth prenatal month is the anteroposterior length of the frontal bone greater than the lateral width. The metopic suture normally closes between two and four years of age. (27)

The diamond-shaped anterior fontanelle is the largest of all fetal fontanelles and is located between the anterosuperior angles and the parietal (Figure 7). This fontanelle normally closes between the age of one and two years. (27)

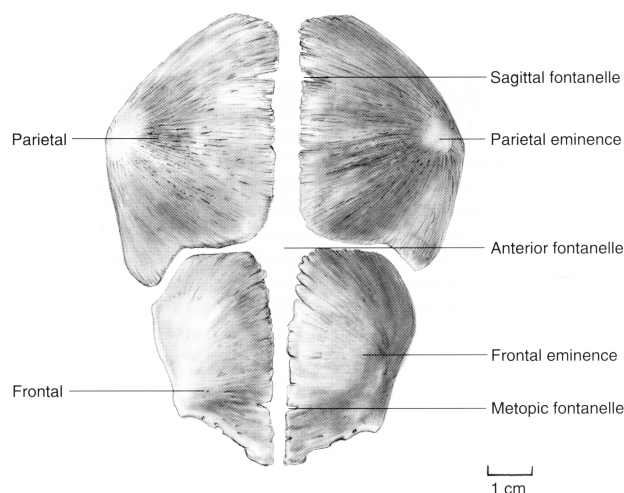


Figure 7: Perinatal frontal and parietal bones. (27)

2.4.4 The zygomatic bone

The zygomatic forms the cheek prominence and separates the orbit from the temporal fossa. It is irregularly shaped and has three surfaces, two processes and five borders. (27) In the eighth prenatal week, one or more centres of ossification arise in the mesenchyme below and lateral to the orbit. These centres fuse in the third month. (5)

By the first half of prenatal life, the zygomatic is recognizable and similar to the adult bone, but has different proportions. (27) At birth the zygomatic is a tri-radiate gracile bone with frontal, temporal and maxillary processes (Figure 8). (27)

During infancy and early childhood the zygomatic bone development has to keep up with the rapid growth of the maxilla, which creates space for the deciduous teeth. This causes an angulation at the notch on the inferior border. (27) The zygomatic receives adult proportions by the time of the eruption of the deciduous dentition. (27)

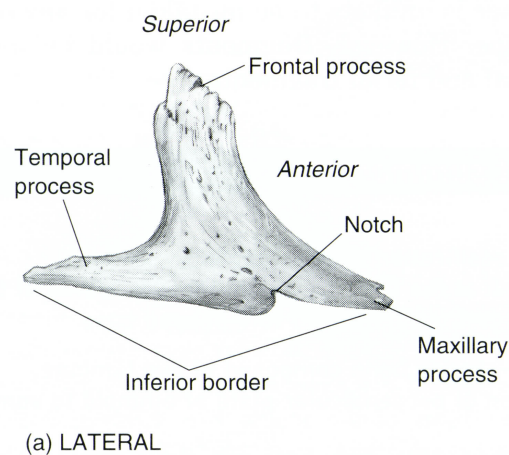


Figure 8: Lateral view of the right perinatal zygomatic bone. (27)

2.4.5 The maxilla

The maxillae form the anterior part of the cranial roof and a large part of the visible surface of the lower face as well as the nasal aperture. Moreover, the maxilla bears all upper teeth. (27) The maxilla develops from the dental bone as the maxillary process of the mandible. It ossifies in the sixth week of prenatal life from six centres that fuse with another by forming two bones. These two bones unite around the fourth lunar month. (5)

In the eleventh week of prenatal life, the crypts of the deciduous incisors start to develop. The crypts of all teeth are completed in the 17th - 18th week of prenatal life (Figure 9). At about one year of age, the formation of the crypt of the second deciduous molar ends and simultaneously the crypt of the first permanent molar is posteriorly opened. After about three years of age the opened socket of the second permanent molar is present. (27)

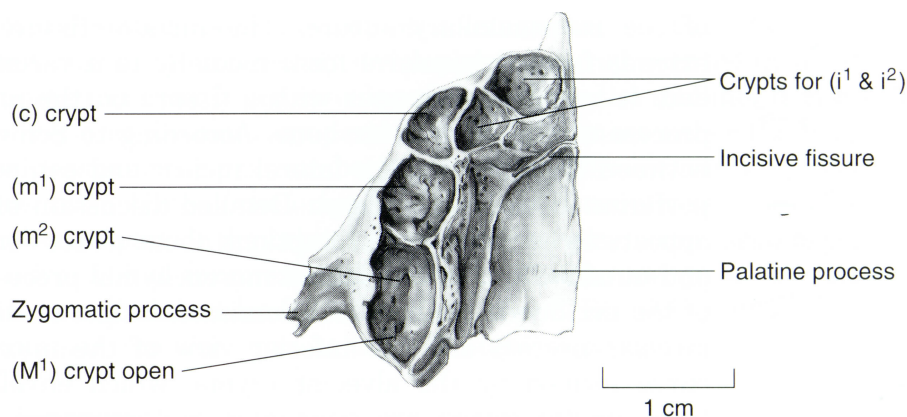


Figure 9: Palatal view of the right maxilla. (27)

2.4.6 The mandible

The mandible is the lower jaw, which is the only skeletal element of the head, apart from the ossicles of the middle ear, that moves independently relative to the cranium. It bears all the lower teeth and is composed of two halves of which each consists of a horizontal body and a vertical ramus (Figure 10). (27)

The ossification of the mandible starts in the mesenchyme, which surrounds the Meckel's cartilage, a cartilaginous bar in the embryonic mandibular arch. This process begins shortly before the ossification of the maxilla. (46) The two halves of the mandible are connected by the symphysis mandibulae (5), a band of connective tissue, which ossifies in the first year of life. (53) The mandibular bony union arises at the age of one or two years starting from one to four centres of ossification. (5)

The shape and proportions of the mandible change significantly during the development. After birth the mandible experiences more variation in shape and increases more in size than any other facial bone. This can be partly explained by the strains of sucking and masticating movements, which play an important role in the development of the final shape of the mandible. (5) Moreover, the mandible has to grow along with the development of the deciduous and permanent dentition, with the changes of size and shape of the maxilla and with the increasing width of the cranial base. (27).

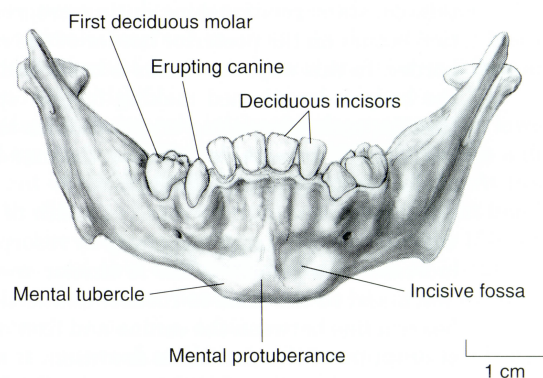


Figure 10: Frontal view of a child's mandible at the dental age of one year. (27)

3 Objectives

The major goal of this study is to evaluate the usefulness of the six proposed skull bone elements for aging young postnatal children. By calculating linear and quadratic regression equations, statements on the predictive aging value of each bone can be made.

Moreover, it is aimed to compare the measurements of the skeletal elements with the data of previous studies by Fazekas & Kósa (1978), Scheuer & MacLauglin-Black (1994), Redfield (1970) and Tocheri & Molto (2002).^(5–8) In this regard, also differences between the dimensions of varying skeletal populations can be examined.

As this study is based on measurements of infants from birth up to two years, it is further aspired to provide a reliable method by the use of regression equations for the estimation of age at death in this age group.

4 Materials and Methods

4.1 Material

The analysed material, a historical collection of skulls from children from the 19th century, was provided by the museum of the dental clinic Vienna. The museum's storage offers three specific osteological collections from the 19th century. One of these was accumulated by Valentin Terzer, a surgeon, dentist and obstetrician. (54)

Valentin Terzer was born on 1st March 1799 in Entiklar, near Kurtatsch in South Tyrol. In 1820 he enrolled as a surgeon of the first class at the University of Vienna and probably worked in a dental practice while studying. In 1834, Valentin Terzer was registered in the list of established surgeons and dentists in Vienna. He is no longer in this medical directory after 1874. According to the baptismal register of his birth-parish in Kurtatsch, Valentin Terzer died on 18th December 1875 in Bozen. (54)

The Terzer collection represents a sample of skulls mostly of the earlier and also the-later childhood - Infans I (up to seven years) and Infans II (up to 14 years) from the year 1833. There are no records about the aim of this historical collection. It is just known that this collection was examined by scientists in the second half of the 19th century and is analysed today by several researchers. (54)

The child corpses of the Terzer collection were received from the Viennese Foundling House, a maternity house or a hospital (Figure 11 and Figure 12). The Viennese Foundling House was built in 1784 by Joseph II to cope with the increasing number of illegitimate births in Vienna. (55) Almost all of these children were either born in the maternity houses or were given directly after birth into this institution. Hence, 70% of the children were already admitted to the Viennese Foundling House at the age of eight or nine days. (55) Although the Viennese Foundling House should serve as a protected place for unmarried women, where they could leave their children, this institution revealed high mortality rates. Until 1813, 97% of all children died. (55)

This fact might be explained by the multitude of people living in a confined space together, by the missing or sparsely respected hygienic rules as well as by the presence of many diseases such as respiratory diseases, diarrhoea or syphilis. (55)



Figure 11: Foundling house in Vienna (Alserstrasse 23) in the first decade of the 20th century. (55)



Figure 12: Transfer of children from the biological mothers to the midwives and the foster mothers. (55)

For the present study 32 skulls of the Terzer collection between the age of seven months in utero and two years, seven months and 22 days were examined (Figure 13 and Figure 14). A few of the skulls of the original Terzer collection had to be excluded due to unknown age at death or missing skull bones. Although not all of the crania were complete, but most of them were in a good state of preservation. Some skulls had additional handwritten information about pathological conditions, age at death, date of death and the individual's names (Table 1). (54)



Figure 13: The analysed individuals of the Terzer collection Part I.



Figure 14: The analysed individuals of the Terzer collection Part II.

Table 1: Individuals of the Terzer collection with information about age at death and cause of death.

Individuum	Age	Notes
P210_ZE-000300	7 months	"The child's head is in the maternity hospital on 27th July 1833. The cesarean section was taken in the seventh month" (MV 71; 4)
P210_ZE-000301	2 months, 28 days	"624/800 ZIERER Maria, 1 month, 28 days, on 14th May 1833 died of emaciation and was brought on 15th of the month" (MV 65; 5)
P210_ZE-000302	3 months, 9 days	"K.M. 58/833 ADEL Josepha, 3 months 9 days, died of Fraisch (epileptic seizures) on 2nd April 1833 "
P210_ZE-000303	3 months, 15 days	MV 73; 6; 10
P210_ZE-000304	3 months, 20 days	"Z.B. 77/833 MÜLLNER Karl, 3 months 20 days died of Fraisch on 11th April" (MV 67; 9)
P210_ZE-000305	4 months, 5 days	"3305/832 EGER Barbara, 4 months 5 days died of hydrocephalus on 1st April 1833" (V.Ö.Z. 19; 12; MV 72; 2)
P210_ZE-000306	9 months, 15 days	V.Ö.Z.; MV 68; 1
P210_ZE-000308	7 months, 13 days	"Z.B. 2771/832 Scheinfeld Franziska, 7 months 15 days died on 14th May 1833 and was brought on 15th of the month" (V.Ö.Z. 26; MV 75; 12)
P210_ZE-000310	4 months, 12 days	"Z.B.nö 34/833 Foundling Streiphnee Sigismund, 4 months 12 days died of Fraisch on 11th May 1833" (MV 69; 10)
P210_ZE-000311	6 months, 28 days	V.Ö.Z. 24; MV 74; 14
P210_ZE-000312	10 months, 17 days	"Gb12 Maria, 10 months 17 days died of paralysis of the lungs on 9th May 1833" (29; MV 76; 15)
P210_ZE-000314	1 year, 17 days	"21/802 Edelmann Joseph, 1 year 17 days died of Fraisch on 1st August 1833" (V.Ö.Z.; 26; MV 83; 33)
P210_ZE-000316	1 year, 4 months, 14 days	"Magdalena Zimmermann Z.b.Nr.: 3129/1831, 1 year 4 months 14 days died of emaciation on 6th April 1833"
P210_ZE-000317	1 year, 5 months, 27 days	"28Gg/831 WURZWALL Karoline, 1 year 5 months 27 days died of emaciation on 23rd April 1833 and was brought on 12th April 1833"
P210_ZE-000318	9 months, 12 days	"Z.B. Ko 1752/833 Binder Karl, 9 months 12 days died of Fraisch on 30th May 1833 and was brought on the same day"
P210_ZE-000319	1 year, 9 months	
P210_ZE-000320	6 months, 15 days	"Z.B.: Nr 2738/833 SELENA Maria, 6 months 15 days died of Fraisch on 11th September 1833"
P210_ZE-000321	5 months, 1 day	
P210_ZE-000322	1 month, 1 day	Skull laterally impressed "959/833 Hauslan Eduard, 1 month 1 day died of hectic fever on 1st April 1833"
P210_ZE-000323	8 months, 2 days	
P210_ZE-000324	17 days	
P210_ZE-000326	4 days	MV 58; 26
P210_ZE-000328	2 months, 14 days	"750/833 Riesenthaler Theresia, 2 months 14 days died of Fraisch on 27th May 1833 and was brought on 28th May 1833"
P210_ZE-000329	8 months, 26 days	"z.B. 2021/832 Kraus Ernst, 8 months 26 days died of measles on 1st April 1833"
P210_ZE-000331	10 months, 1 day	
P210_ZE-000332	1 year, 6 months	open skull (V.Ö.Z. 37; MV 86; 29)
P210_ZE-000333	1 year, 4 months	open skull (V.Ö.Z. 38; 30; MV 87; 31)
P210_ZE-000334	1 year, 9 months, 8 days	"Nr1900/831 Tischler Johann, 1 year 9 months 8 days died of Fraisch on 10th May 1833" (MV 90; 36)
P210_ZE-000335	1 year, 10 months, 10 days	V.Ö.Z. 42; 34; MV 91; 37
P210_ZE-000336	1 year, 11 months	active caries (V.Ö.Z. 43; 35; MV 92; 28)
P210_ZE-000337	2 years, 7 months, 22 days	MV 93; 38; 36
P210_ZE-000338	1 year, 8 months	caries (MV 88; 35)

4.2 Methods

4.2.1 Description of the measurements of all analysed skull bones

The children's skulls were measured with a sliding caliper in millimetres. The dimensions of the following six bones were examined:

1. The occipital bone (squama occipitalis, pars basilaris os occipitalis)
2. The parietal bone
3. The frontal bone
4. The zygomatic bone
5. The maxilla
6. The mandible

The following 15 dimensions of the skull bones (Table 2) were measured according to the specifications by Fazekas & Kósa (1978) and Schaefer, Black & Scheuer (2009) and are verbally as well as graphically described in the following subchapters.(5,56)

Table 2: Summary of all measurements taken.

Measurements at fetal skulls			
1	Occipital squama height	Squama occipitalis	The occipital bone
2	Occipital squama width		
3	Maximum width basilaris	Pars basilaris	
4	Sagittal length basilaris		
5	Maximum length basilaris		
6	Parietal height	The parietal bone	
7	Parietal width		
8	Frontal height	The frontal bone	
9	Frontal width		
10	Zygomatic length	The zygomatic bone	
11	Zygomatic width (oblique height)		
12	Maxilla length	Maxilla	
13	Mandible body length	Mandible	
14	Mandible width (of the arc of the mandible)		
15	Full length of the half mandible (oblique length)		

All of the following definitions for the measurements have been adopted verbatim from Fazekas & Kósa (1978) and Schaefer, Black & Scheuer (2009). (5) (56)

The squama occipitalis

1. Occipital squama height

The distance measured in the midline, from the posterior border of the foramen magnum to the tip of the squama. (5)

Straight line distance from the posterior border of the foramen magnum to the tip of the squama. (56)

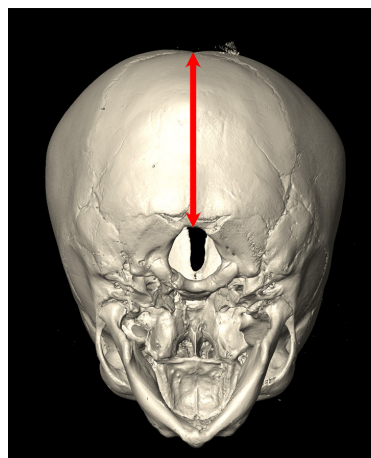


Figure 15: The height of the occipital squama.

2. Occipital squama width

The greatest width of the occipital squama in the line of the sutura mendosa. (5)

Straight line distance from the greatest width of the occipital squama in the line of the sutura mendosa. (55)

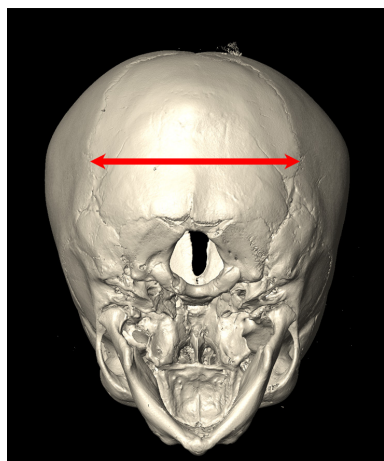


Figure 16: The width of the occipital squama.

The pars basilaris os occipitalis

3. Maximum width basilaris

The greatest distance measured in the line of the lateral tubercles. (5)

Greatest distance measured in the line of the lateral angles. (56)

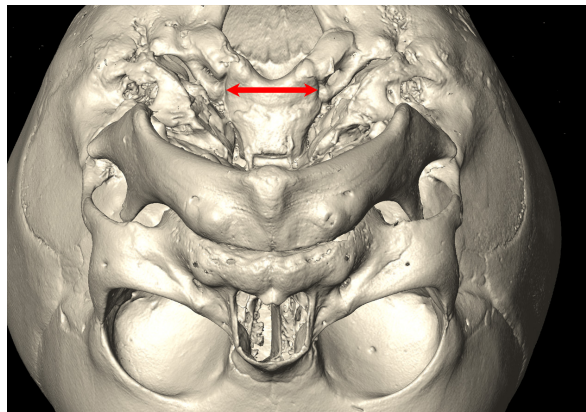


Figure 17: The maximum width of the pars basilaris occipitalis.

4. Sagittal length basilaris

Midline distance between the foramen magnum and synchondrosis sphenooccipitalis. (56)

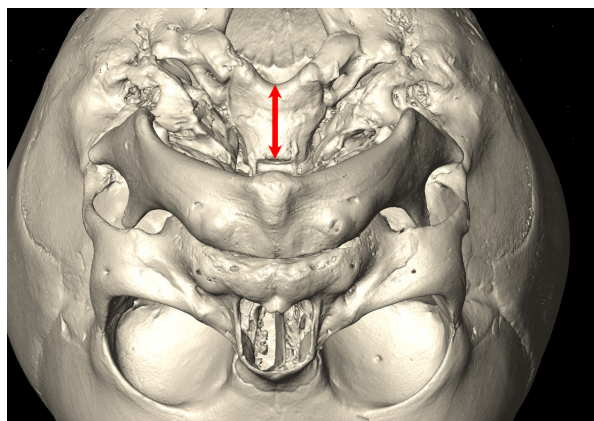


Figure 18: The sagittal length of the pars basilaris occipitalis.

5. Maximum length basilaris

The distance measured in the midline between the foramen magnum and synchondrosis sphenoccipitalis. (5)

Maximum distance between the posterior edge of the lateral condyle and the synchondrosis sphenoccipitalis (56)

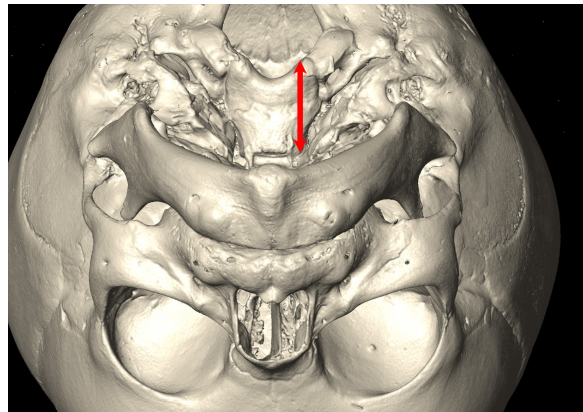


Figure 19: The maximum length of the pars basilaris occipitalis.

The parietal bone

6. Height

The distance (length) measured parallel with the coronal suture, from the middle of the squamous margin to the middle of the sagittal margin, across the tuber parietal eminence. (5)

Straight line distance from midsquamous border to midsagittal border across parietal eminence parallel to coronal suture. (56)

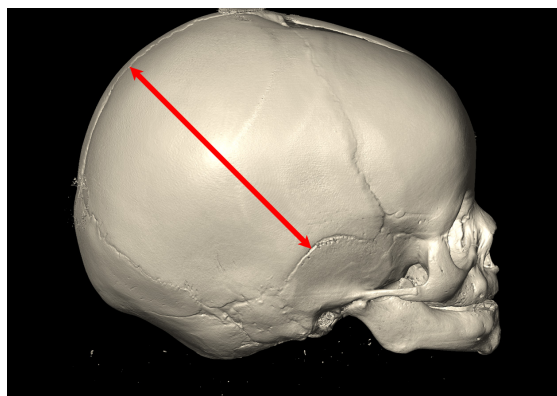


Figure 20: The height of the parietal bone.

7. Width

The distance measured parallel with the sagittal suture between the frontal and the occipital margins across the parietal eminence. (5)

Straight line distance from frontal to occipital borders across parietal eminence, parallel to sagittal suture. (56)

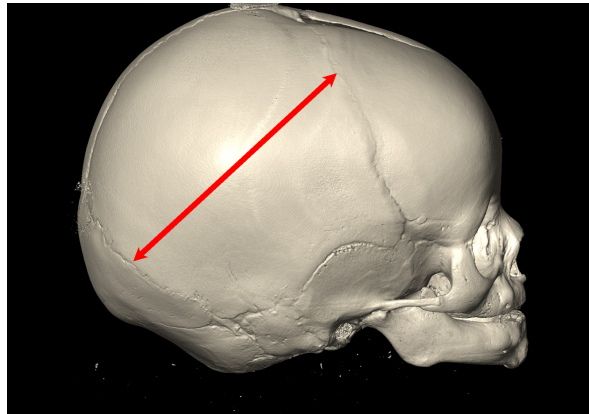


Figure 21: The width of the parietal bone.

The frontal bone

8. Height

The distance (length) measured from the middle of the superior margin of the orbit, across the frontal eminence to the superior peak of the frontal bone. (5)

Straight-line distance from middle of the superior margin of the orbit to superior peak of bone across frontal eminence. (56)

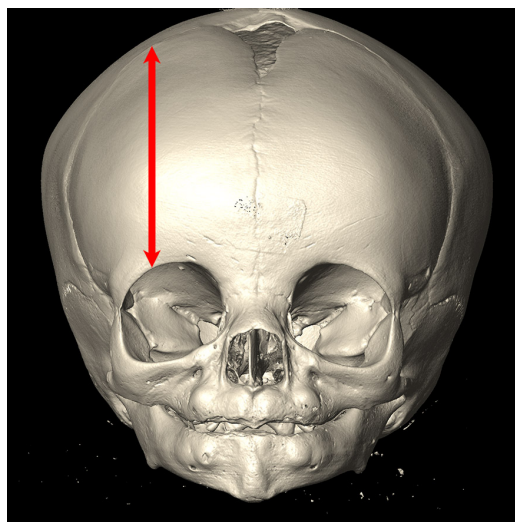


Figure 22: The height of the frontal bone.

9. Width

In younger fetuses (3 to 3 ½ lunar months) the distance measured at the level of the superior border of the orbit. In fetuses older than 4 lunar months the distance measured transversally at the level of the frontal eminence. (5)

Straight-line distance from width across frontal eminence at right angles to length (width at superior border of orbit in younger fetuses). (56)

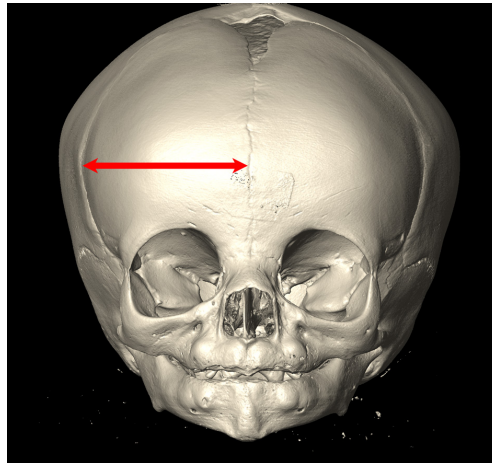


Figure 23: The width of the frontal bone.

The zygomatic bone

10.Length

The distance measured between the anterior end of the infraorbital margin (marginal process) and the posterior end of the temporal process. (5)

Anterior end of maxillary process to posterior end of temporal process. (56)

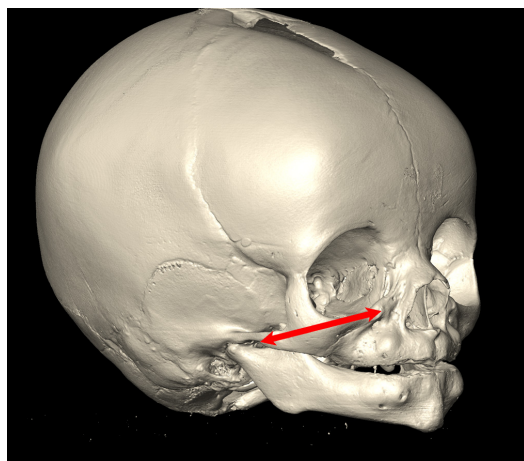


Figure 24: The length of the zygomatic bone.

11. Width (oblique height)

The distance measured between the anterior end of the infraorbital margin (marginal process) and the frontosphenoidal process. (5)

Anterior end of maxillary process to superior end of frontal process. (56)

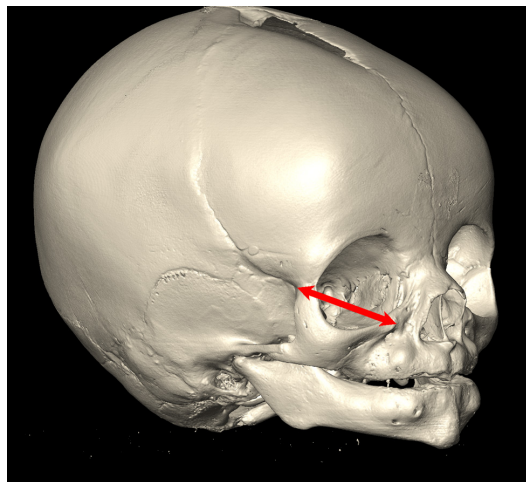


Figure 25: The width (oblique height) of the zygomatic bone.

The maxilla

12. Length

The sagittal measurement of the maxilla between the anterior nasal process and the posterior border of the palatal process. (5)

Anterior nasal spine to posterior border of palatal process in sagittal plane. (56)

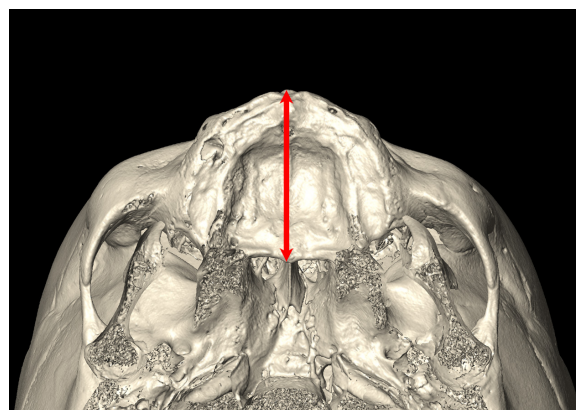


Figure 26: The length of the maxilla.

The mandible

13. Body length

The distance from the tuberculum mentale to the ipsilateral angle. (5)

From tuberculum mentale to mandibular angle. (56)

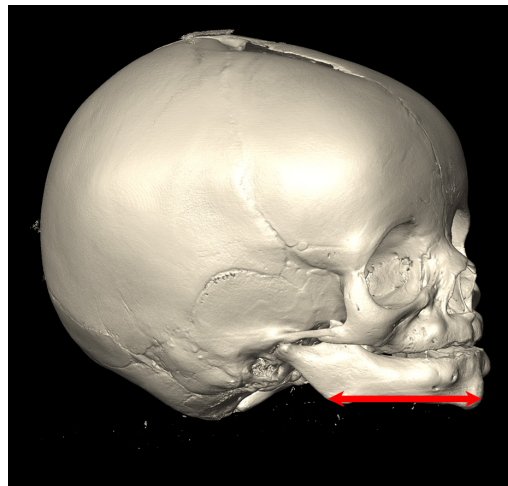


Figure 27: The body length of the mandible.

14. Width (of the arc of the mandible)

The distance measured between the coronoid and condyloid process. (5)

Posterior border of condyle to tip of coronoid process. (56)

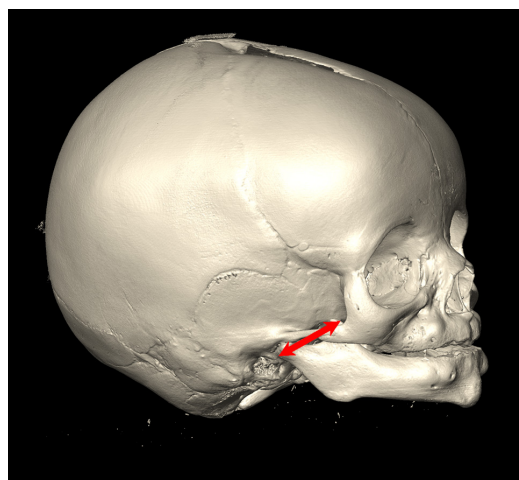


Figure 28: The width of the mandible.

15. Full length of the half mandible (oblique length)

The distance measured between the tuberculum and the head of the mandible of the same side. (5)

From tuberculum mentale to posterior border of condyle. (56)

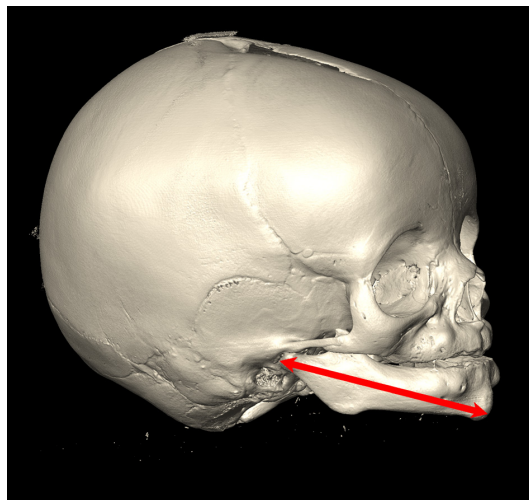


Figure 29: The full length of the half mandible (oblique length).

4.2.2 Statistical analysis

For the statistical evaluation the program R version 3.2.2 (57) has been used. The graphics were created with ggplot2. (58) Descriptive statistics include values such as the mean, the median, the standard deviation (SD) as well as the minimum and the maximum of each dimension measured.

For inductive statistics linear models, ordinary least square models and second order polynomial regression models have been applied for predicting age. Thereby the prediction error was assessed using the Standard Error of Estimate (S.E.E.), the Mean Absolute Deviation (M.A.D.) and the Leave-one-out-cross-validation (CV error). (59)

An adjusted R-squared (R^2 = coefficient of determination) variable was determined to demonstrate the strength of the association between the age (in days on y-axis) and the skull dimensions (in mm on x-axis) in a linear and a quadratic regression analysis. (60) If the R^2 value is near one or at least higher than 0.7 the relation is strong and linear or quadratic. If the value is near zero or at least less than 0.5, the relation is far from being linear or quadratic. (5)

5 Results

The results include descriptive statistics of the measurements taken on the 32 skulls of the Terzer collection. In addition, scatter plots illustrate the calculated linear (marked in red) and quadratic (marked in blue) regression equations. For each equation the S.E.E., the M.A.D., the adjusted R-squared (R^2) and the CV error are provided.

5.1 Descriptive statistics

The mean value (Mean), standard deviation (SD), minimum (Min.), median, maximum (Max.), number of individuals (n) and the missing skeletal dimensions of the bone (missing) of every skeletal dimension are given in Table 3.

The mean age of all analysed individuals is 307.8 days, which equals 10.1 months (Table 3, first row). A standard deviation of +/- 252.3 days indicates an age variance of the sample between 55.5 and 560.1 days. The median sums up to 235.5 days. As according to Jukic et al. (2013) the median time from ovulation to birth is 268 days (61), hence the minimum age in this study is -55.0 days (= 213 days - 268 days; skull ZE-000300, 7 months in utero). The maximum value represents the age of the oldest individual, which is two years, seven months and 22 days (ZE-000337).

The same values (mean, SD, min, max, median) are given for each dimension in millimetres.

Table 3: Descriptive statistics of the measurements.

	Mean	SD	Min	Median	Max	n	Missing
Age	307.8	252.3	−55.0	235.5	965.0	32	0
ChordHeightParsSquamaOccipital	67.1	11.6	48.9	66.7	88.2	32	3
ChordWidthParsSquamaOccipital	70.0	12.8	47.1	68.3	92.9	32	3
MaxWidthParsBasilarisOccipital	14.5	3.0	8.1	14.1	24.2	32	0
SagittalLengthParsBasilarisOccipital	11.7	1.9	8.3	11.5	16.6	32	0
MaxLengthParsBasilarisOccipital	15.7	2.5	11.2	15.6	23.2	32	0
ChordHeightParietal	81.5	11.2	60.1	82.4	101.4	32	3
ChordWidthParietal	86.0	13.5	62.7	84.2	117.0	32	3
ChordHeightFrontal	58.8	9.7	45.1	57.3	85.9	32	3
ChordWidthFrontal	51.2	7.1	34.8	50.2	68.3	32	4
LengthZygomatic	27.2	4.8	17.0	27.1	39.5	32	2
ObliqueHeightWidthZygomatic	21.1	3.4	14.2	20.8	27.9	32	2
LengthMaxilla	28.7	3.2	21.6	28.3	37.0	32	1
BodyLengthMandible	40.4	6.1	29.1	39.5	57.2	32	0
WidthMandible	16.1	2.8	10.4	16.1	24.5	32	2
ObliqueLengthMandible	58.1	10.1	37.5	55.7	82.7	32	1

5.2 Regression models

5.2.1 The chord height of the pars squama occipitalis

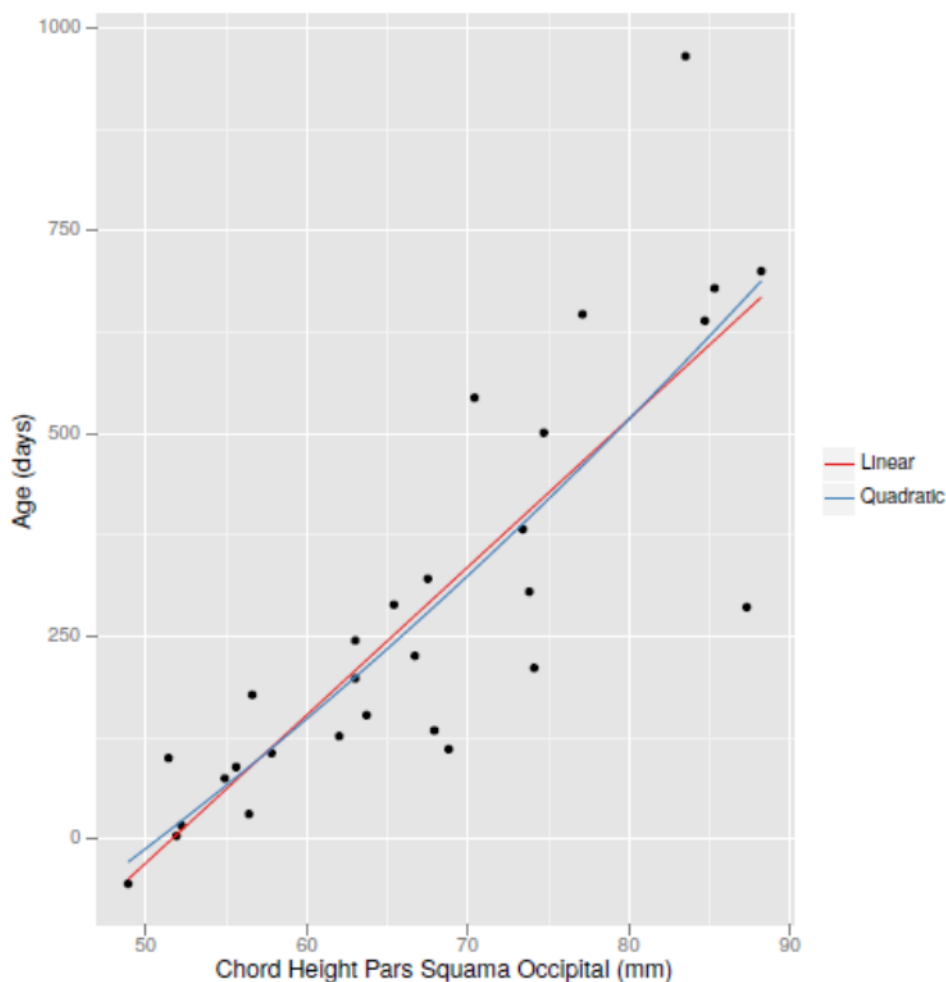


Figure 30: Linear and quadratic regressions of the chord height of the pars squama occipitalis.

The quadratic (blue line) and the linear (red line) regression equation have the same R^2 value of 0.71. The M.A.D. for the linear regression is with 90.23 days slightly larger than the quadratic regression (88.48 days). Table 4 summarizes these values in addition to the CV error and the S.E.E. for each equation.

Table 4: Model assessment for the chord height of the pars squama occipitalis.

model	S.E.E.	M.A.D.	R^2	CV Error
Age = $-941.8 + 18.3 \cdot X$	134.04	90.23	0.71	147.59
Age = $-567.5 + 7 \cdot X + 0.1 \cdot X^2$	133.63	88.48	0.71	155.80

5.2.2 The chord width of the pars squama occipitalis

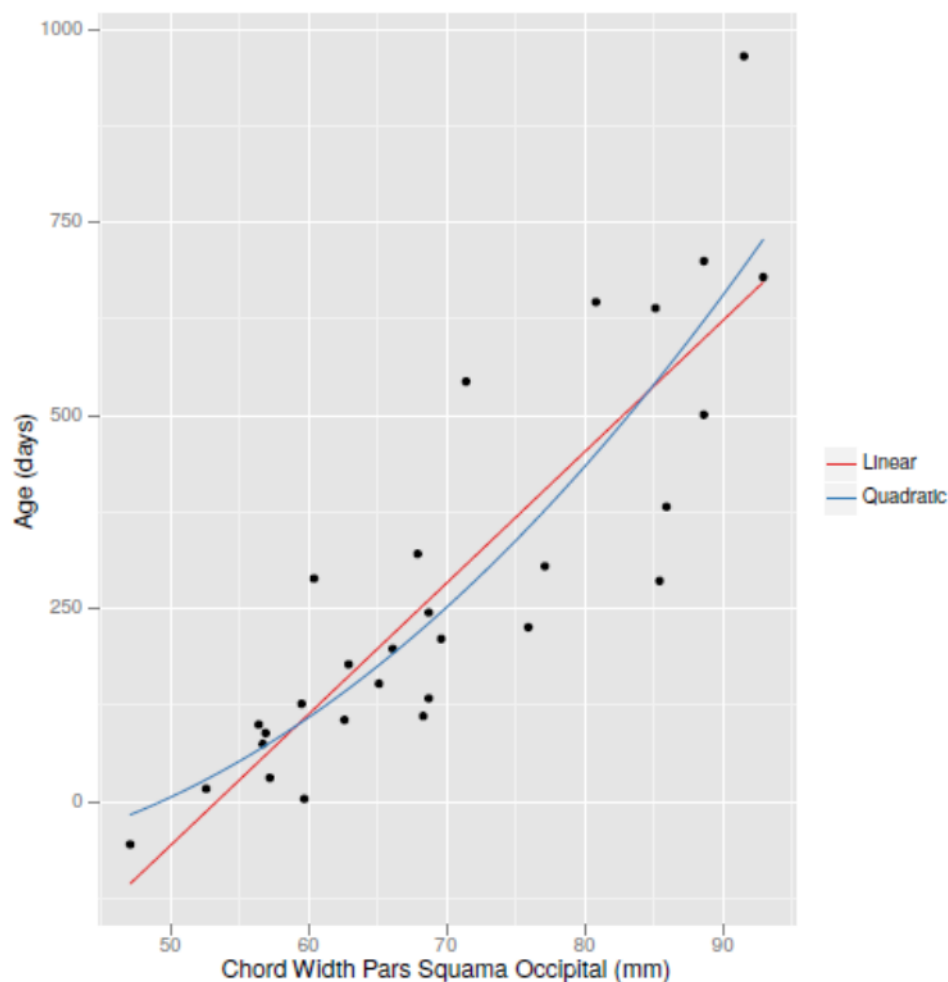


Figure 31: Linear and quadratic regressions of the chord width of the pars squama occipitalis.

The quadratic (blue line) regression equation has a marginally higher R^2 value of 0.76 compared to the linear (red line) regression equation (0.75). This is also reflected by the smaller M.A.D. for the quadratic regression (90.81 days) than for the linear regression (M.A.D. 96.14 days). Table 5 summarizes these values in addition to the CV error and the S.E.E. for each equation.

Table 5: Model assessment for the chord width of the pars squama occipitalis.

model	S.E.E.	M.A.D.	R^2	CV Error
$\text{Age} = -906.8 + 17 \cdot X$	124.50	96.14	0.75	135.45
$\text{Age} = 81.9 - 11.4 \cdot X + 0.2 \cdot X^2$	120.92	90.81	0.76	136.10

5.2.3 The maximum width of the pars basilaris occipitalis

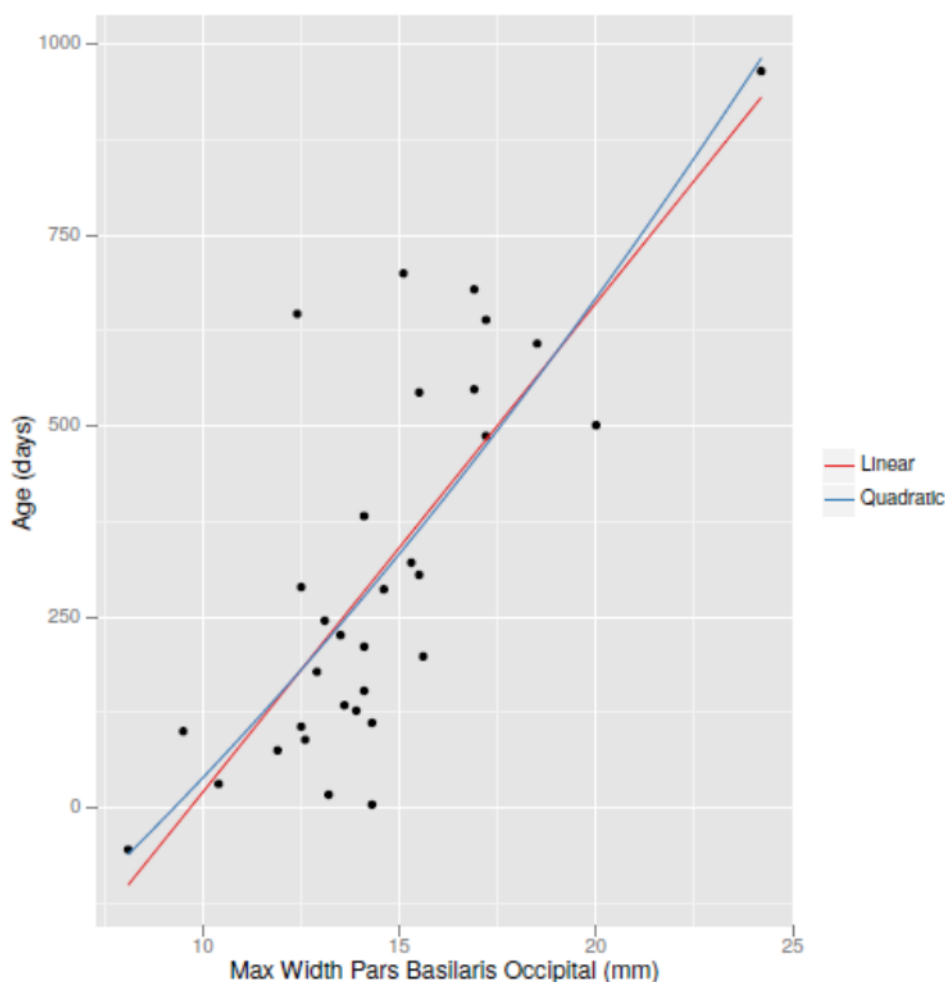


Figure 32: Linear and quadratic regressions of the maximum width of the pars basilaris occipitalis.

R^2 has a minimally higher value in the quadratic (blue line; 0.60) than in the linear regression equation (red line; 0.59). Both, show better M.A.D. values (quadratic: 118.00 days; linear: 120.54 days) than the calculations by Scheuer and MacLaughlin-Black (1994; M.A.D. 266.30 days), which are presented together with the CV Error and the S.E.E. for each equation in Table 6.

Table 6: Model assessment and comparison with Scheuer & MacLaughlin-Black, 1994, for the maximum width of the pars basilaris occipitalis.

model	S.E.E.	M.A.D.	R^2	CV Error
Age = $-620.6 + 64.1 \cdot X$	158.30	120.54	0.59	165.99
Age = $-421.8 + 37.7 \cdot X + 0.8 \cdot X^2$	157.70	118.00	0.60	167.05
ScheuerMclaughlinBlack	332.82	266.30		332.82

5.2.4 The sagittal length of the pars basilaris occipitalis

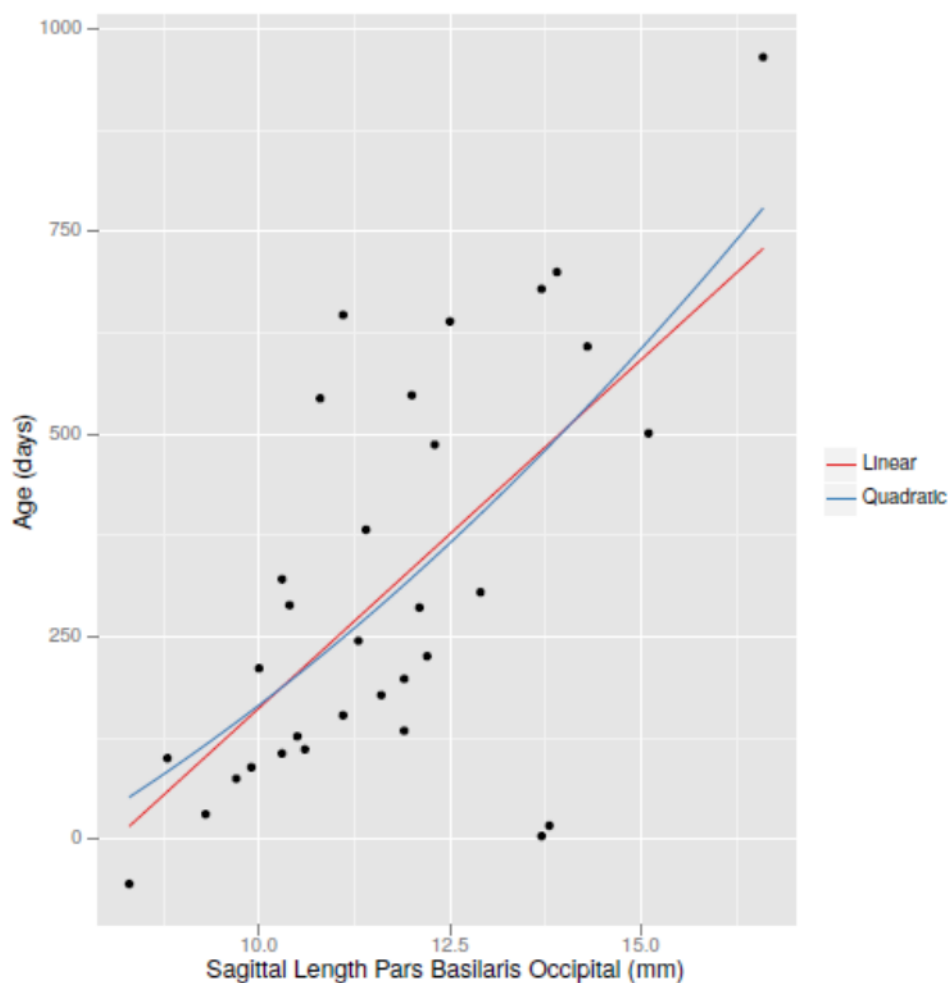


Figure 33: Linear and quadratic regressions of the sagittal length of the pars basilaris occipitalis.

The R^2 of both, the linear (red line) and quadratic (blue line) regression equation has the same value of 0.41. Also the M.A.D. values are quite similar, with the quadratic regression (M.A.D. 151.30 days) showing the lower value than the linear regression (M.A.D. 152.32 days). The calculations by Scheuer and MacLaughlin-Black (1994) indicate an M.A.D. of 262.56 days. Table 7 summarizes these values in addition to the CV Error and the S.E.E. for each equation.

Table 7: Model assessment and comparison with Scheuer & MacLaughlin-Black, 1994, for the sagittal length of the pars basilaris occipitalis.

model	S.E.E.	M.A.D.	R^2	CV Error
Age = $-696.6 + 85.9 \cdot X$	191.47	152.32	0.41	205.55
Age = $-241.8 + 9.3 \cdot X + 3.1 \cdot X^2$	190.95	151.30	0.41	221.39
ScheuerMacLaughlinBlack	325.87	262.56		325.87

5.2.5 The maximum length of the pars basilaris occipitalis

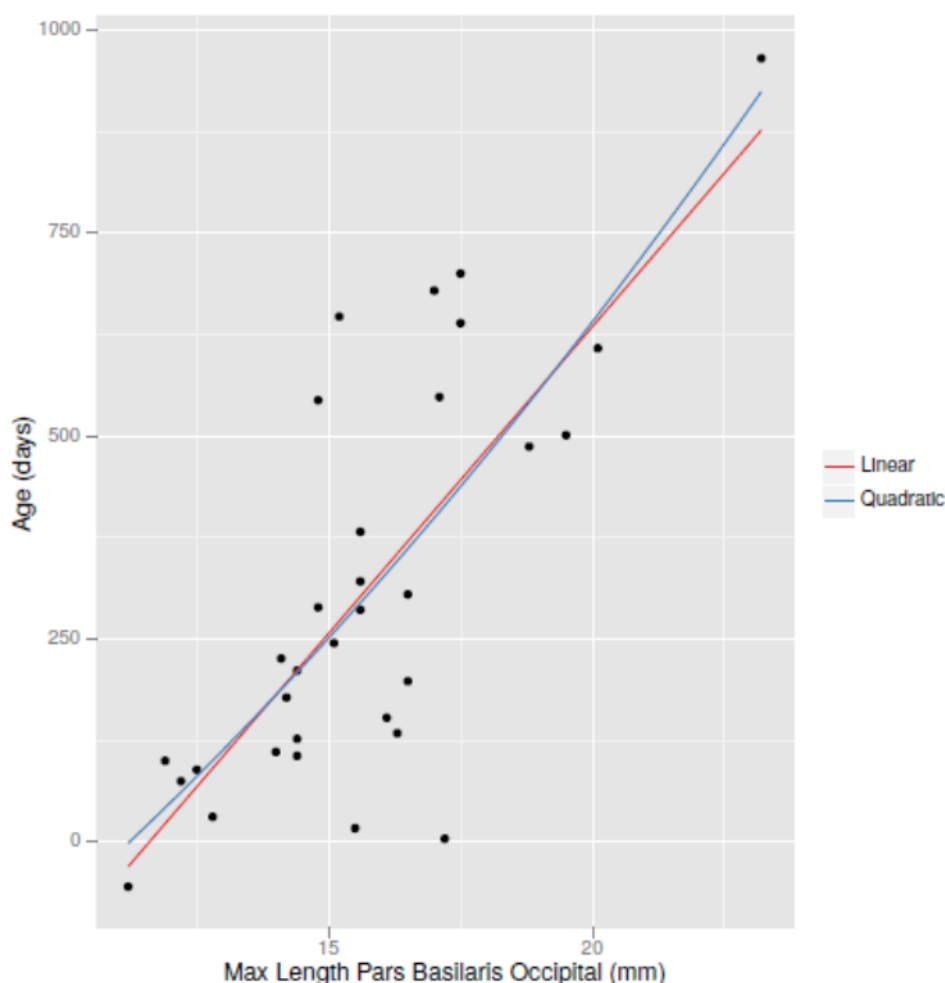


Figure 34: Linear and quadratic regressions of the maximum length of the pars basilaris occipitalis.

The quadratic (blue line) regression equation has an R^2 of 0.57, which is slightly higher than that of the linear (red line) regression equation (0.56). Of both, the quadratic regression (M.A.D. 118.75 days) and the linear regression (M.A.D. 120.51 days) the M.A.D. values are much lower than the value obtained by Scheuer and MacLaughlin-Black (1994; M.A.D. 265.86). Table 8 summarizes these values in addition to the CV Error and the S.E.E. for each equation.

Table 8: Model assessment and comparison with Scheuer & MacLaughlin-Black, 1994, for the maximum length of the pars basilaris occipitalis.

model	S.E.E.	M.A.D.	R^2	CV Error
Age = $-876.6 + 75.6 \cdot X$	164.21	120.51	0.56	171.87
Age = $-528 + 32.5 \cdot X + 1.3 \cdot X^2$	163.73	118.75	0.57	175.43
ScheuerMclaughlinBlack	337.61	265.86		337.61

5.2.6 Comparison of the length of the pars basilaris vs. the width of the pars basilaris

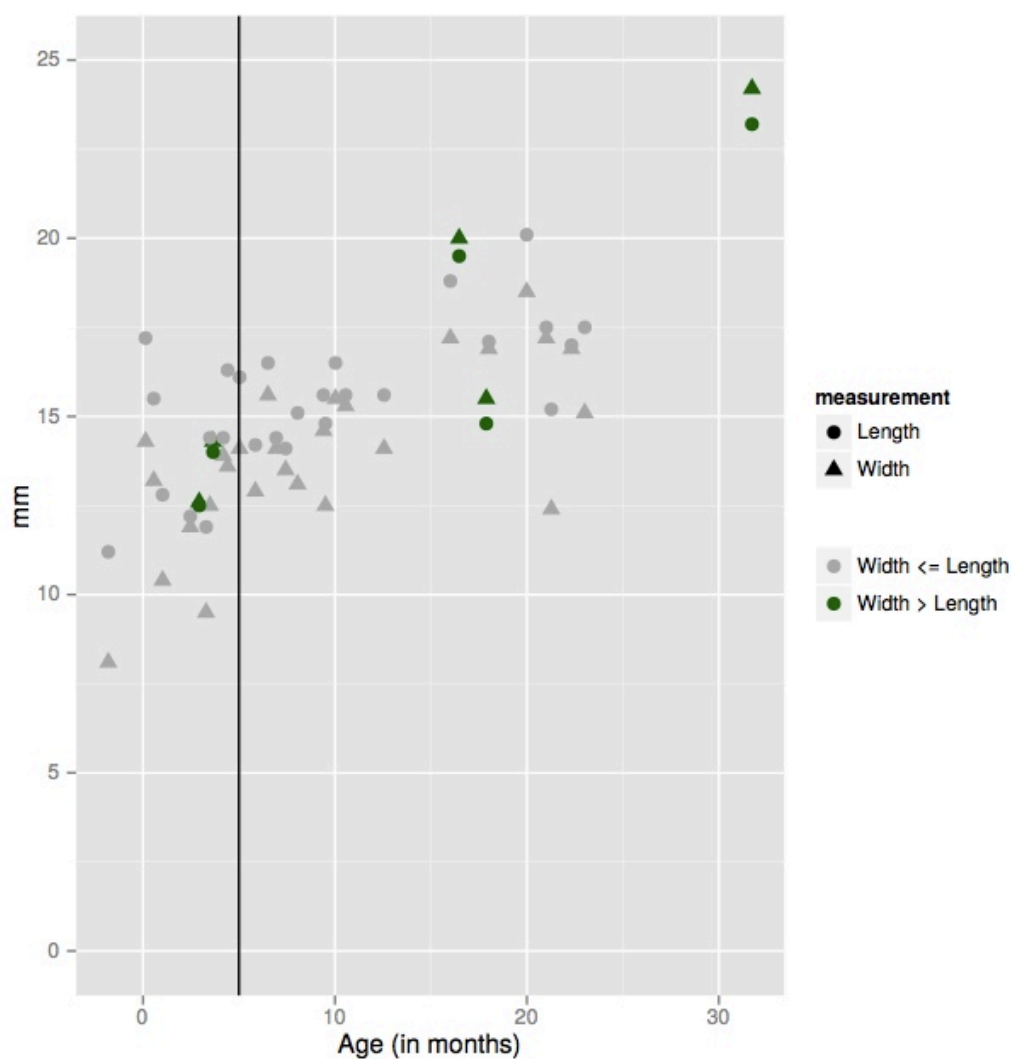


Figure 35: Relationship between the maximum width and the maximum length of the pars basilaris.

Figure 35 shows the relationship between the maximum width (triangles) and the maximum length (circles) of the pars basilaris of this study. The black line indicates the age of five months postpartum. The green marked dots (= maximum length) and triangles (= maximum width) represent the individuals where the width exceeds the length of the pars basilaris.

5.2.7 The chord height of the parietal bone

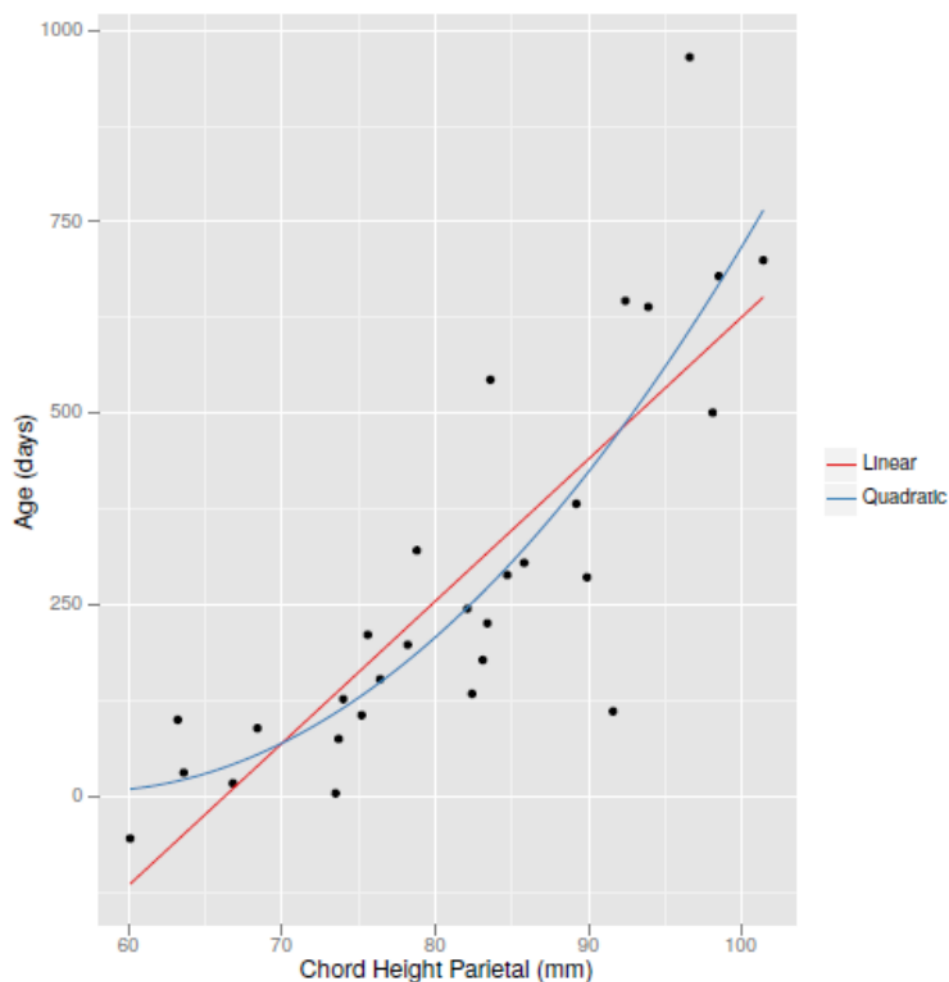


Figure 36: Linear and quadratic regressions of the chord height of the parietal bone.

The quadratic (blue line) regression equation has a higher R^2 value (0.73) than the linear (red line) regression equation (0.68). Also, a considerably smaller M.A.D. for the quadratic regression (87.67 days) compared to the linear regression (M.A.D. 104.99 days) is present. Table 9 summarizes these values in addition to the CV Error and the S.E.E. for each equation.

Table 9: Model assessment for the chord height of the parietal bone.

model	S.E.E.	M.A.D.	R^2	CV Error
Age = $-1229.2 + 18.5 \cdot X$	138.91	104.99	0.68	150.12
Age = $1285.4 - 44.7 \cdot X + 0.4 \cdot X^2$	128.99	87.67	0.73	142.88

5.2.8 The chord width of the parietal bone

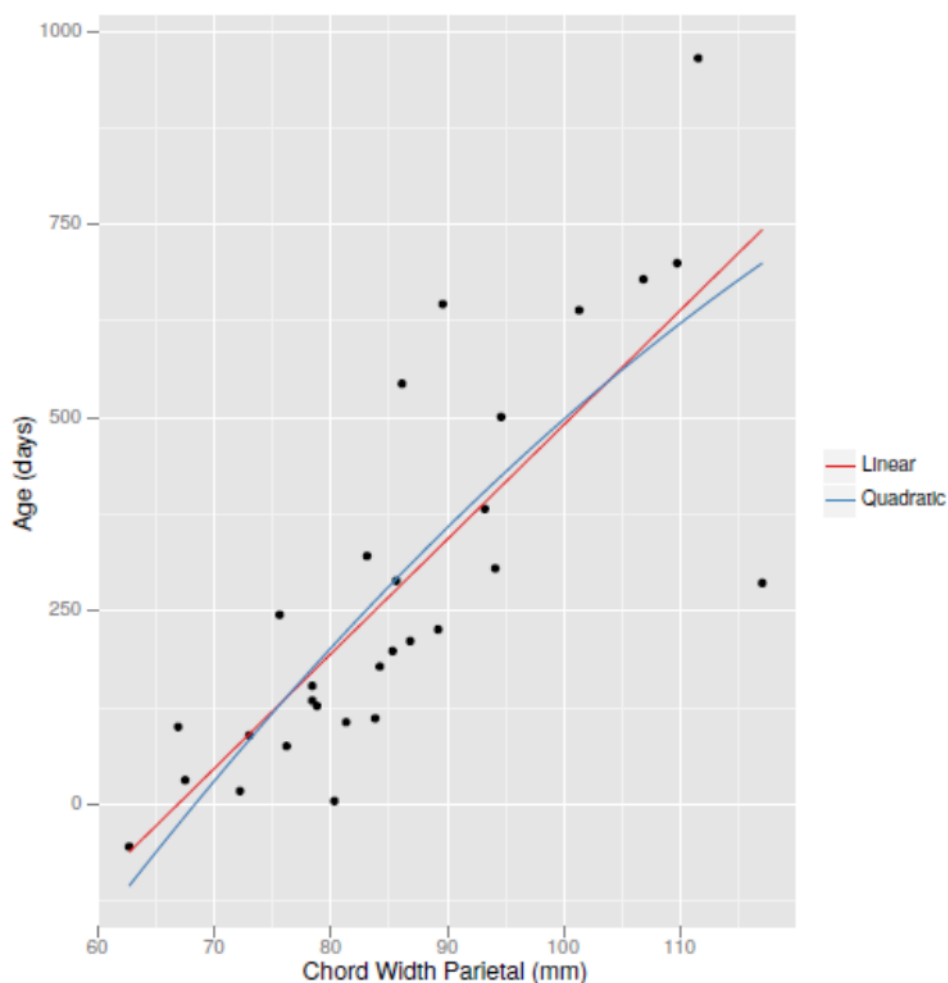


Figure 37: Linear and quadratic regressions of the chord width of the parietal bone.

Both, the quadratic (blue line) regression equation and the linear (red line) regression equation have similar R^2 values of 0.64 and 0.63, respectively. The M.A.D. for the quadratic regression (114.26 days) is higher than the linear regression (M.A.D. 108.97 days). Table 10 summarizes these values in addition to the CV Error and the S.E.E. for each equation.

Table 10: Model assessment for the chord width of the parietal bone.

model	S.E.E.	M.A.D.	R^2	CV Error
Age = $-992 + 14.8 \cdot X$	149.96	108.97	0.63	172.57
Age = $-1620.2 + 29.1 \cdot X - 0.1 \cdot X^2$	148.98	114.26	0.64	199.33

5.2.9 The chord height of the frontal bone

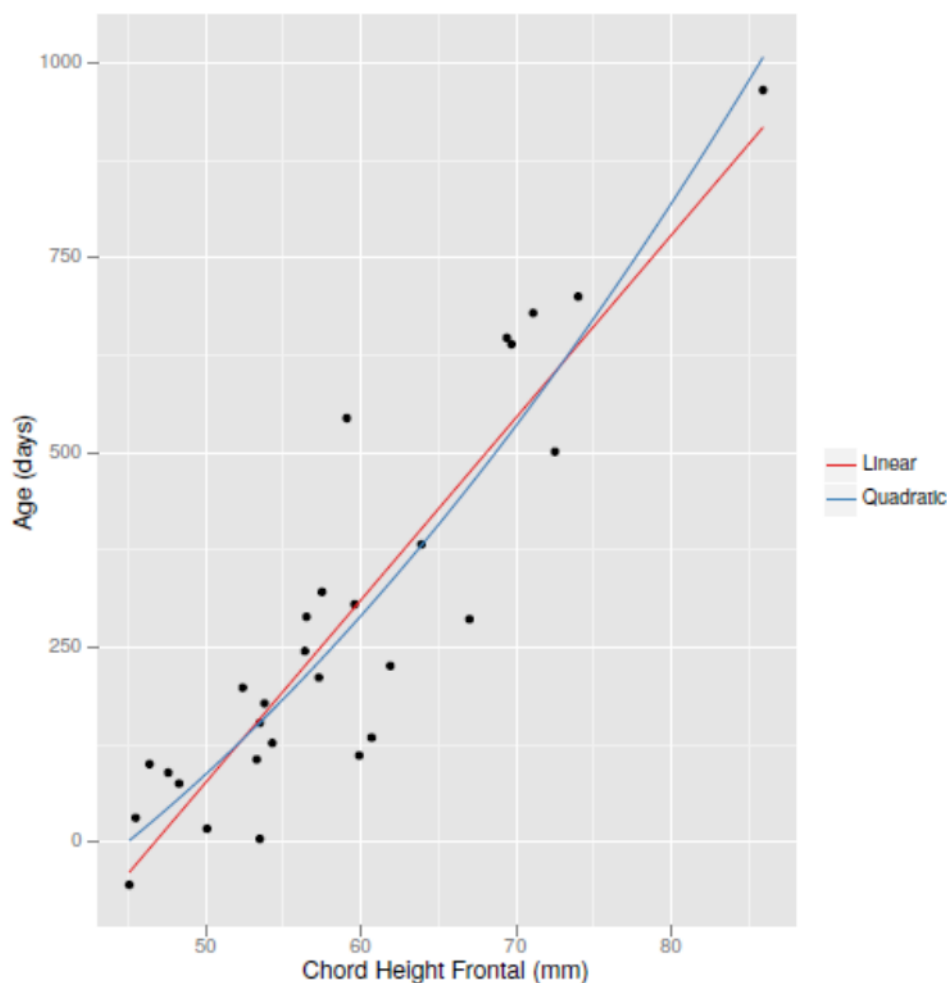


Figure 38: Linear and quadratic regressions of the chord height of the frontal bone.

R^2 for the quadratic (blue) regression equation (0.83) is similar to that of the linear (red) regression equation (0.82). The M.A.D. for the quadratic regression (79.53 days) is slightly smaller than that of the linear regression (M.A.D. 82.68 days). Table 11 summarizes these values in addition to the CV Error and the S.E.E. for each equation.

Table 11: Model assessment for the chord height of the frontal bone.

model	S.E.E.	M.A.D.	R^2	CV Error
$\text{Age} = -1095.7 + 23.4 \cdot X$	104.11	82.68	0.82	110.28
$\text{Age} = -317.7 - 2.1 \cdot X + 0.2 \cdot X^2$	101.17	79.53	0.83	113.80

5.2.10 The chord width of the frontal bone

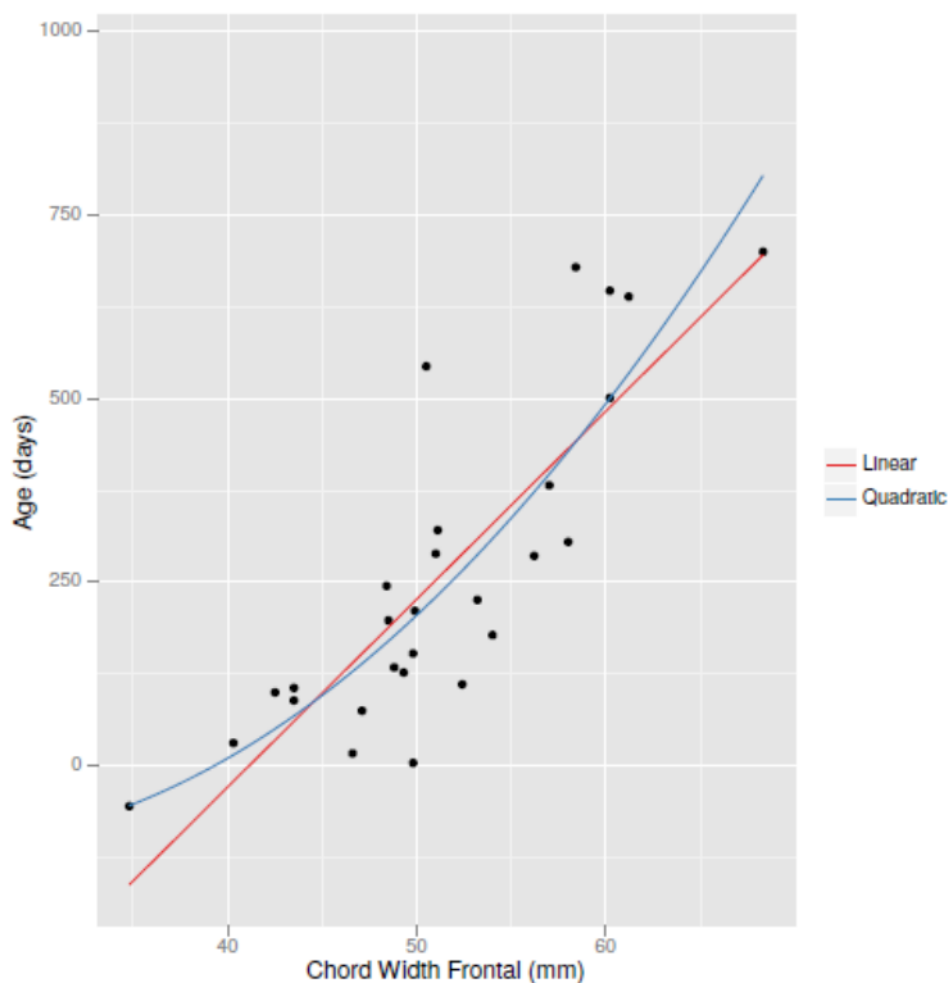


Figure 39: Linear and quadratic regressions of the chord width of the frontal bone.

The quadratic (blue) regression equation has an R^2 of 0.72, which is slightly higher than that of the linear (red) regression equation (0.70). The value of the M.A.D. for the quadratic regression (85.88 days) is much lower than that of the linear regression (M.A.D. 93.54 days). Table 12 summarizes these values in addition to the CV Error and the S.E.E. for each equation.

Table 12: Model assessment for the chord width of the frontal bone

model	S.E.E.	M.A.D.	R^2	CV Error
$\text{Age} = -1053.2 + 25.6 \cdot X$	118.38	93.54	0.70	126.10
$\text{Age} = 164.6 - 22.5 \cdot X + 0.5 \cdot X^2$	113.44	85.88	0.72	129.49

5.2.11 The length of the zygomatic bone

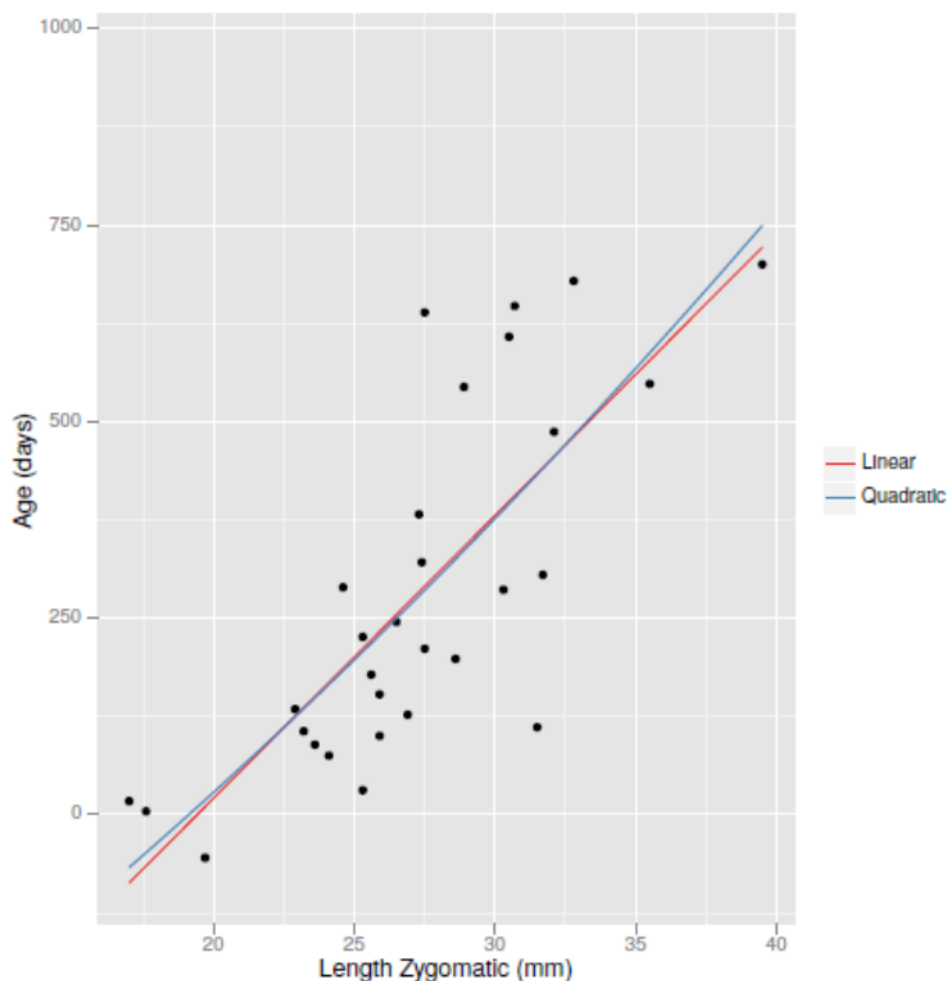


Figure 40: Linear and quadratic regressions of the length of the zygomatic bone.

The R^2 of both, the linear (red) and quadratic (blue) regression equation has the same value of 0.60. Also the M.A.D. values are quite similar, with the quadratic regression (M.A.D. 110.79 days) showing the lower value than the linear regression (M.A.D. 111.04 days). Table 13 summarizes these values in addition to the CV Error and the S.E.E. for each equation.

Table 13: Model assessment for the length of the zygomatic bone.

model	S.E.E.	M.A.D.	R^2	CV Error
Age = $-698.4 + 36 \cdot X$	141.22	111.04	0.60	149.07
Age = $-532.1 + 23.5 \cdot X + 0.2 \cdot X^2$	140.99	110.79	0.60	152.68

5.2.12 The oblique height (width) of the zygomatic bone

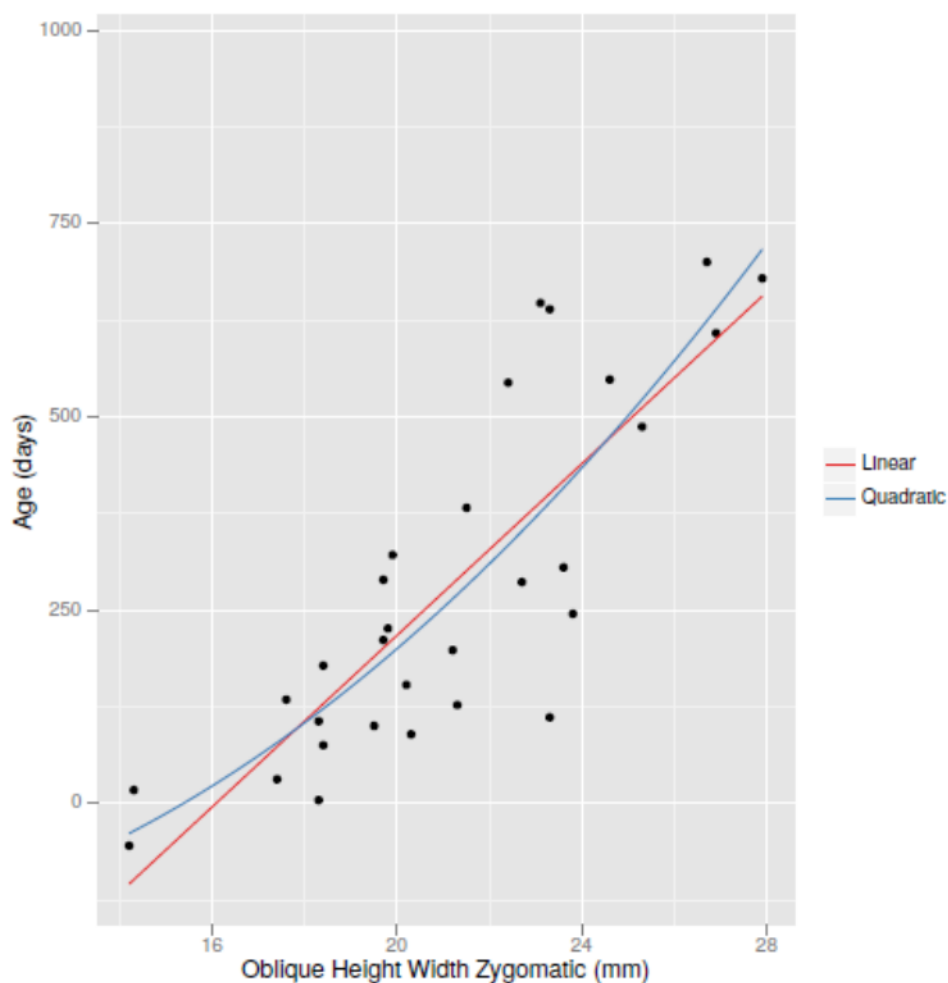


Figure 41: Linear and quadratic regressions of the oblique height (width) of the zygomatic bone.

The quadratic (blue) regression equation has an R^2 of 0.71, which is slightly higher than that of the linear (red) regression equation (0.69). The value of the M.A.D. for the quadratic regression (95.36 days) is much lower than that of the linear regression (M.A.D. 98.70 days). Table 14 summarizes these values in addition to the CV Error and the S.E.E. for each equation.

Table 14: Model assessment for the oblique height (width) of the zygomatic bone.

model	S.E.E.	M.A.D.	R^2	CV Error
$\text{Age} = -892.6 + 55.5 \cdot X$	122.70	98.70	0.69	129.66
$\text{Age} = -124.5 - 19 \cdot X + 1.8 \cdot X^2$	120.08	95.36	0.71	128.27

5.2.13 The length of the maxilla

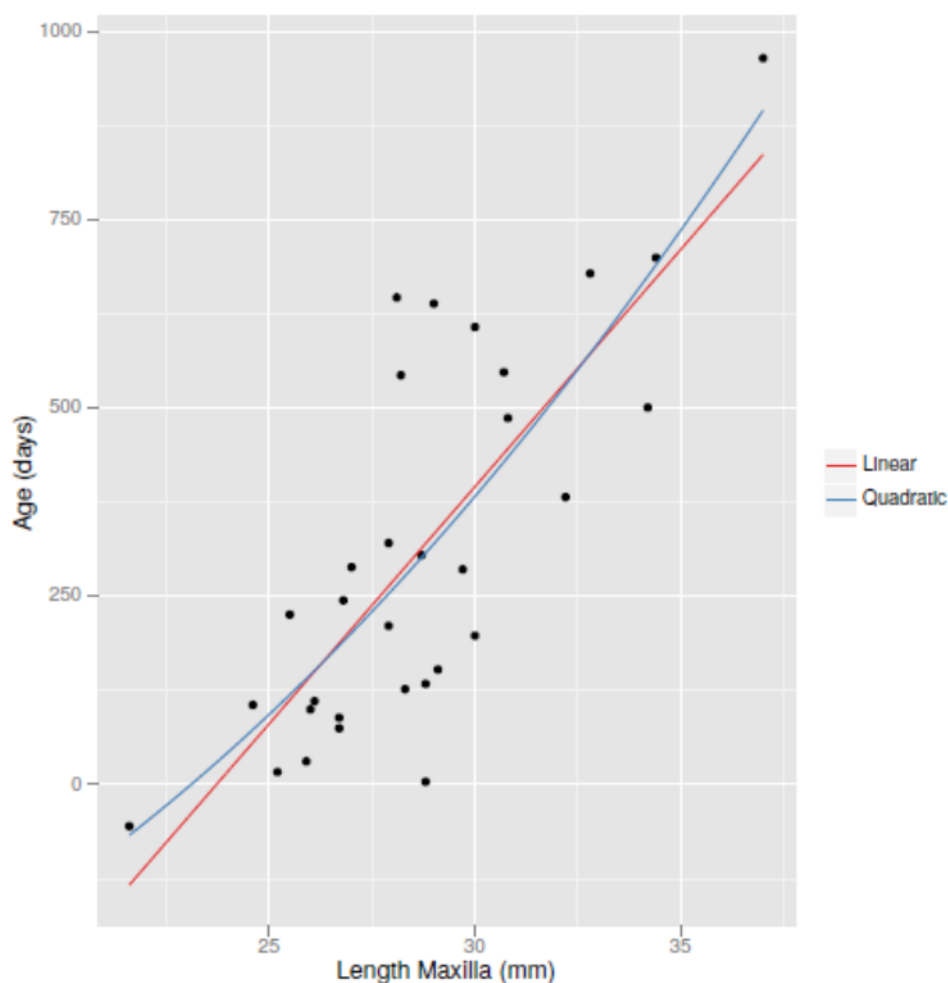


Figure 42: Linear and quadratic regressions of the length of the maxilla.

R^2 for the quadratic (blue) regression equation (0.62) is similar to that of the linear (red) regression equation (0.61). The M.A.D. for the quadratic regression (123.77 days) is slightly smaller than that of the linear regression (M.A.D. 128.54 days). Table 15 summarizes these values in addition to the CV Error and the S.E.E. for each equation.

Table 15: Model assessment for the length of the maxilla.

model	S.E.E.	M.A.D.	R^2	CV Error
Age = $-1493.6 + 63 \cdot X$	156.41	128.54	0.61	164.80
Age = $-396.8 - 12.3 \cdot X + 1.3 \cdot X^2$	155.27	123.77	0.62	166.42

5.2.14 The body length of the mandible

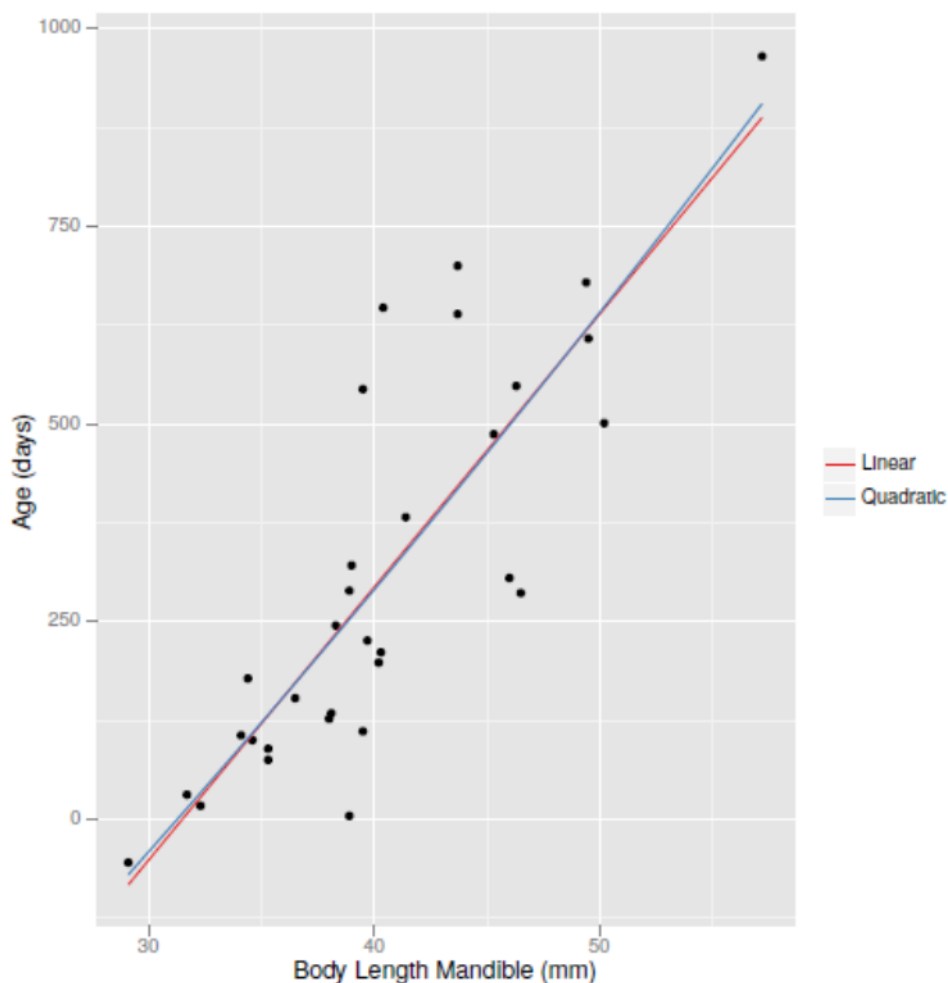


Figure 43: Linear and quadratic regressions of the body length of the mandible.

The linear (red) and quadratic (blue) regression equation have the same R^2 value of 0.70. Also the M.A.D. values are quite similar, with the quadratic regression (M.A.D. 98.09 days) showing the lower value than the linear regression (M.A.D. 98.87 days). Table 16 summarizes these values in addition to the CV Error and the S.E.E. for each equation.

Table 16: Model assessment for the body length of the mandible.

model	S.E.E.	M.A.D.	R^2	CV Error
$\text{Age} = -1087.9 + 34.5 \cdot X$	135.52	98.87	0.70	142.19
$\text{Age} = -920.9 + 26.4 \cdot X + 0.1 \cdot X^2$	135.44	98.09	0.70	147.14

5.2.15 The width of the mandible

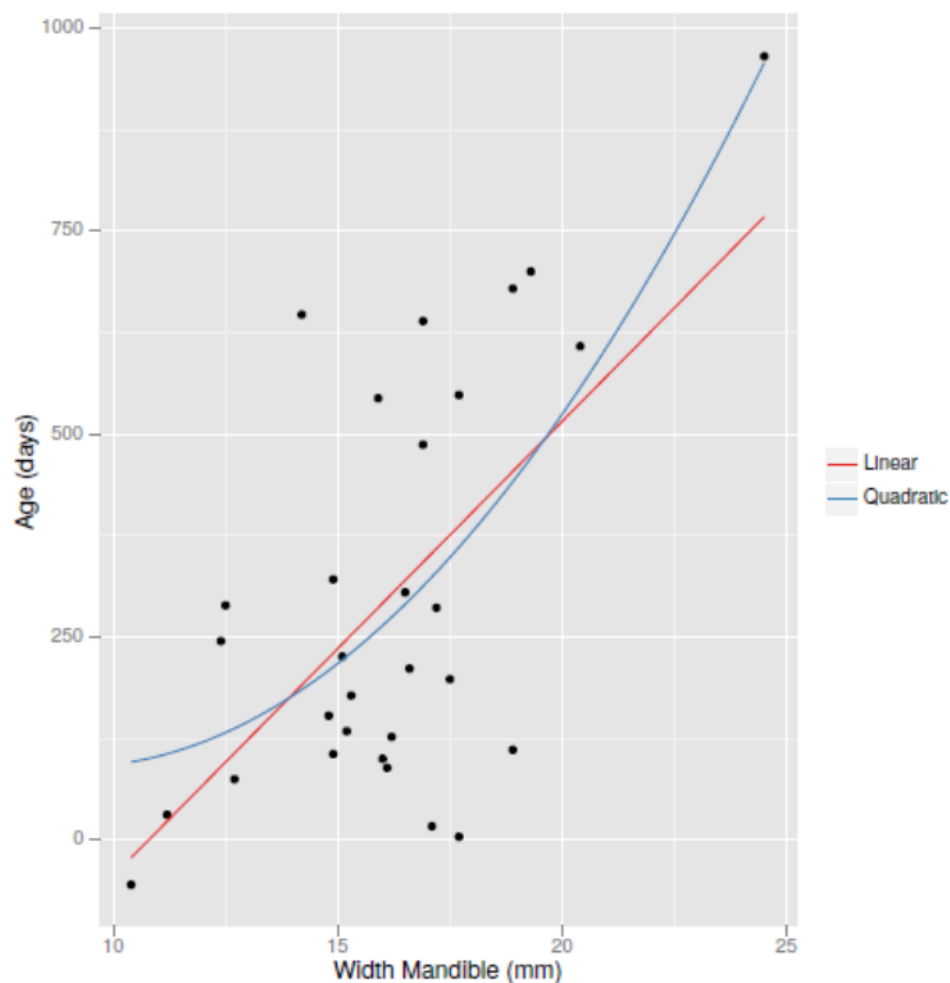


Figure 44: Linear and quadratic regressions of the width of the mandible.

The quadratic (blue) regression equation has an R^2 of 0.41, which is slightly higher than that of the linear (red) regression equation (0.38). The value of the M.A.D. for the quadratic regression (157.36 days) is much lower than that of the linear regression (M.A.D. 165.36 days). Table 17 summarizes these values in addition to the CV Error and the S.E.E. for each equation.

Table 17: Model assessment for the width of the mandible.

model	S.E.E.	M.A.D.	R^2	CV Error
$\text{Age} = -603.9 + 56 \cdot X$	200.29	165.36	0.38	214.31
$\text{Age} = 391.8 - 66.4 \cdot X + 3.7 \cdot X^2$	194.05	157.36	0.41	208.41

5.2.16 The oblique length of the mandible

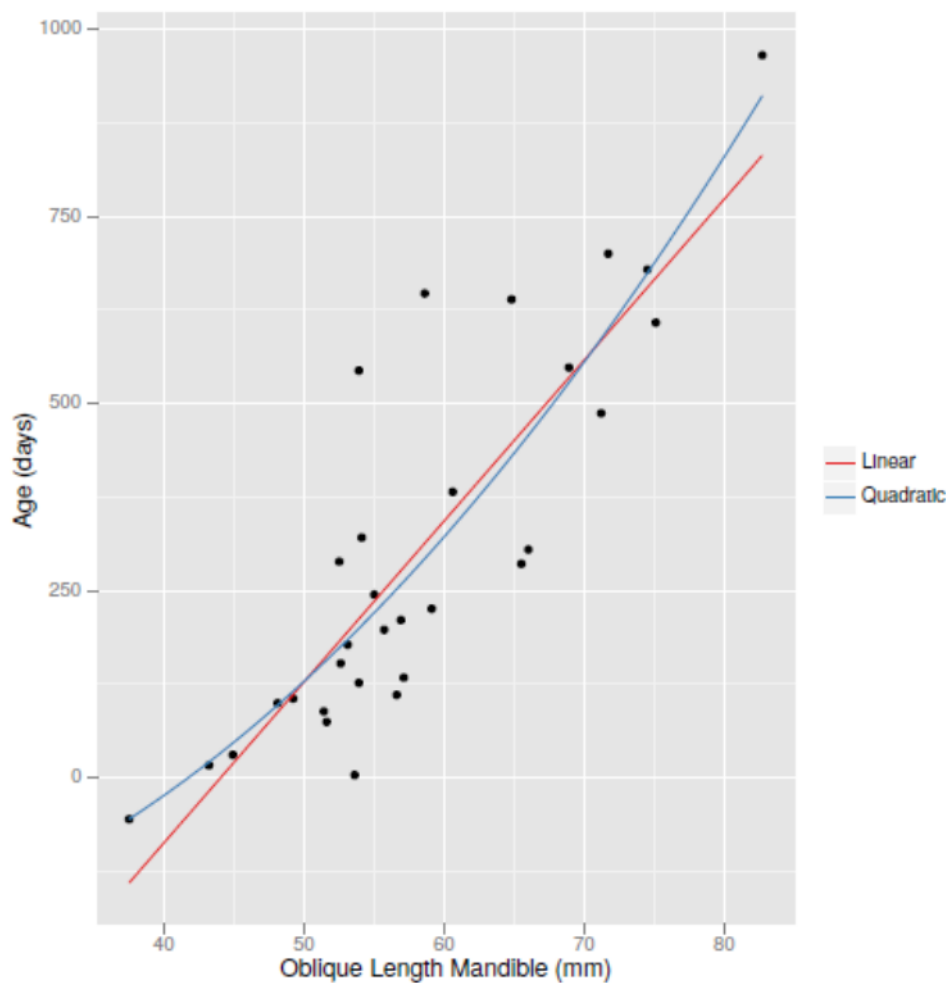


Figure 45: Linear and quadratic regressions of the oblique length of the mandible.

R^2 for the quadratic (blue) regression equation (0.74) is similar to that of the linear (red) regression equation (0.73). The M.A.D. for the quadratic regression (89.94 days) is slightly smaller than that of the linear regression (M.A.D. 98.26 days). Table 18 summarizes these values in addition to the CV Error and the S.E.E. for each equation.

Table 18: Model assessment for the oblique length of the mandible.

model	S.E.E.	M.A.D.	R^2	CV Error
$\text{Age} = -945.6 + 21.5 \cdot X$	129.19	98.26	0.73	136.46
$\text{Age} = -227 - 3 \cdot X + 0.2 \cdot X^2$	126.48	89.94	0.74	134.93

Table 19 below shows all values of R^2 of the linear and quadratic regressions arranged in a descending magnitude.

Table 19: Measurements sorted by the value of R^2 of linear and quadratic regression.

Bone measurement	Linear regression R^2	Bone measurement	Quadratic regression R^2
Frontal bone chord height	0.82	Frontal bone chord height	0.83
Pars squama occipitalis chord width	0.75	Pars squama occipitalis chord width	0.76
Mandible longest oblique length	0.73	Mandible longest oblique length	0.74
Pars squama occipitalis chord height	0.71	Parietal bone chord height	0.73
Frontal bone chord width	0.7	Pars squama occipitalis chord height	0.72
Mandible body length	0.7	Frontal bone chord width	0.71
Zygomatic bone width	0.69	Zygomatic bone width	0.71
Parietal bone chord height	0.68	Mandible body length	0.7
Parietal bone chord width	0.63	Parietal bone chord width	0.64
Maxilla length	0.61	Maxilla length	0.62
Zygomatic bone length	0.6	Zygomatic bone length	0.6
Pars basilaris occipitalis max. width	0.59	Pars basilaris occipitalis max. width	0.6
Pars basilaris occipitalis max. length	0.56	Pars basilaris occipitalis max. length	0.57
Pars basilaris occipitalis sagittal length	0.41	Pars basilaris occipitalis sagittal length	0.41
Mandible width	0.38	Mandible width	0.41

6 Discussion

The determination of age at death of human skeletal remains is an important subject for the forensic anthropology (10) (62) (63) as it can provide a lot of relevant information for the identification of individuals. For this reason it is necessary to find those measurements which are most effective for aging skeletal remains of infants depending on their varying states of preservation. Especially skeletons of fetuses and early juveniles often do not survive the burial unscathed. (7) As bones of the skull have the advantage that they are better represented and preserved in a burial environment (40), age estimation of young infants could be based on these skeletal elements.

The aim of this study was to analyse which bones of the skull are best suited for the estimation of age at death of very young postnatal children. Moreover, our data was compared to the measured dimensions and age-predictions of fetal and juvenile skeletal skull elements from previous studies. Another goal was to establish generally applicable regression equations for skull bones and to test if they are good indicators for the determination of age at death.

In the scope of this study the historical Terzer collection from the 1830's was analysed. Valentin Terzer, a surgeon, dentist and obstetrician, collected approximately 40 skulls of infants from foundling houses, maternity houses and hospitals. (54) Of these, 32 skulls have been examined in this thesis, which ranged in their age from seven months in utero to two years, seven months and 22 days. From all skulls 15 measurements on the frontal, parietal, occipital, zygomatic, mandible and maxilla were taken with a sliding caliper.

The following subchapters should give an overview of the most and least appropriate skull measurements for aging of infants in this study.

6.1 The most and least suitable measurements of this study

For a classification into the most and least appropriate measurements, the adjusted R-squared (R^2) is the best suitable indicator (Table 19) and will therefore serve as the basis for the ranking and interpretation. R^2 depicts the strength of association between the individual skull bone measurement (x-axis) and the age (y-axis). (60) If the R^2 value is near one or at least higher than 0.7 the relation is strong, whereas if the value is near zero or at least less than 0.5 the relation is far from being strong. (5) The values of R^2 in this study range between 0.38 and 0.83. Those measurements with an R^2 above 0.7 seem to reveal a good relation to age and will therefore more specifically discussed below. The measurements with R^2 values below 0.7 might rather be of poor predictive value for age of infants as characterized in the next chapters. As the quadratic regression generally showed a better correlation with age and a provided a better description of the data, the adjusted R-squared of the quadratic regression is used for the following interpretations.

6.1.1 Measurements best suited for the estimation of age at death

The **chord height of the frontal bone** was the measurement best suited for the estimation of age at death in this study (Figure 38). R^2 has a high value of 0.83 (Table 11) and therefore this dimension would be a good indicator for age determination. In addition, the **chord width of the pars squama occipitalis** has a relatively high R^2 of 0.76 (Table 5 and Figure 31). Hence, if the pars squama of the occipital bone is found unbroken, it is a useful and reliable measurement for the estimation of age at death. Also, the **oblique length of the mandible** is a good indicator for the estimation of age at death (Figure 45). R^2 has a value of 0.74 (Table 18).

6.1.2 Measurements least suited for the estimation of age at death

All measurements along the **pars basilaris occipitalis** were amongst the least suited measurements for the estimation of age at death in this study. The value of R^2 varied between 0.41 and 0.60 (Table 6 - 8). Hence, for this study it was not a measurement that provided a good prediction of age at death in infants. The **width of the mandible** showed the lowest value of R^2 of 0.41 (Table 17). As also many outliers were found, it was the least appropriate measurement for the estimation of age at death.

6.1.3 The regression equations

The results provide new regression equations for 15 skull measurements for children from birth up to 2.5 years. These might constitute a good basis for further work in forensic and archaeological fields when applied for sub-adults.

6.2 Factors influencing the reliability of age estimation

The current study examined documented skeletal remains of infants. The skulls of the children have been obtained from the Viennese Foundling House in the year 1833. This institution was hardly able to fulfil the requirements for responsible and professional childcare, did not have enough rooms for the children and until the 1890's the morgue was located between inhabited rooms. (64) Most of the children suffered from diseases, which were due to the bad sanitary conditions, inadequate nutrition, forms of neglect and abuse. Only the strongest children survived. (64)

Due to the preserved handwritten leaflets deposited inside of the skulls of 16 of the infants it is known of which diseases they died (Table 1). Most of them succumbed to "Fraisen" and emaciation, which are obsolete terms for epileptic seizures and tuberculosis. Nevertheless it can be assumed that the other children also died of similar diseases.

That the children's background might be of relevance shows a comparison of the pars basilaris measurements obtained in this study with those by Tocheri and Molto (2002), Redfield (1970) as well as by Scheuer and MacLaughlin-Black (1994). (8)(6)(7) Individuals of this thesis showed for all three measurement smaller values than those of the other studies. In general, the skulls of the "Terzer" sample had smaller dimensions compared to previously published samples.

Also the samples used for comparison might have a different structure, e.g. the age of individuals might not cover the same age range and the statistical procedures chosen might not be comparable. All these additional factors can also lead to different outcomes in different studies.

6.3 Interpretation of the results of this study in comparison to previously published data

6.3.1 Mandible

In a morphometric study of the mandible of 65 fetuses between 22 and 40 weeks of amenorrhea conducted by Minier et al., regression equations on the relation between fetal age and mandible measurements were created. The dimension that best correlated with age was the mandible width ($R^2 > 0.72$). (13)

The fact that the mandibular measurements (oblique length and width) show up amongst both, the least as well as the best suited measurements for the estimation of age, might be explained as follows: The mandible is one of the first bones that starts to ossify. (65) After birth the mandible experiences more variation in shape and increases more in size than any other facial bone. The mandible has to grow along with the development of the deciduous and permanent dentition, with the changes of size and shape of the maxilla and with the increasing width of the cranial base. (27)

One important change is that the ramus of the mandible becomes more vertical in adulthood. (13) Bareggi et al. mentioned that the mandibular ramus grows relatively faster than the body. (66) This may be the reason why the oblique length of the mandible might be a good age indicator. Therefore this measurement of the mandible has been used for the estimation of age and sex in the field of forensic anthropology. (65)

One reason, why the width of the mandible is the least suited measurement could be, that the height of the mandible increases more than the width, i.e. the latter shows a slower postnatal growth. Moreover, it shows some of the smallest values of all the measurements taken. This might be relevant insofar, as small dimensions possibly do also undergo only small changes in size during the development. These again might be a confounding factor in the estimation of age, because larger changes in size may lead to regression equations that perform better.

6.3.2 Frontal bone, zygomatic bone, maxilla and pars squama occipitalis

To our knowledge, these four skull elements were not used for age determination studies in postnatal infants before. However, the results of this thesis suggest, that some of these dimensions might provide a good basis for age estimation analyses in young infants.

6.3.3 Pars basilaris occipitalis

Scheuer and MacLaughlin-Black (1994), Fazekas and Kósa (1987), Redfield (1970), Tocheri and Molto (2002) and Nagaoka et al. (2012) describe, that the basilar part of the occipital bone is a useful indicator for the estimation of age at death. (5–8,10)

This is not in accordance with our study, as here the measurements of the pars basilaris were found amongst the dimensions that are least useful in the determination of age at death. They showed comparatively low R^2 from 0.41 to 0.60.

Also the application of the results of these previous studies to the “Terzer” sample did not show convincing results. This might be mainly explained by the differences in the social, geographical background and historical affiliation of the study samples.

Scheuer and MacLaughlin-Black (1994) measured the pars basilaris occipitalis of 64 fetal and juvenile skeletons from the St. Bride and Spitalfields collection in the UK. (7) When applying these standards to estimate the age of the individuals of the “Terzer” sample the results are very poor (Tables 6 – 8). The age estimates obtained using the Scheuer & MacLaughlin-Black method were very high. Moreover, the M.A.D. shows that their determination of age at death differed by +/- 260 days, which is much higher than those achieved by applying the regression equations developed in this thesis (approx. +/-120 days).

Also, Fazekas and Kósa (1978) measured the length and width of the pars basilaris occipitalis of 138 human fetuses from the third to the tenth lunar month. (5) Redfield (1970) analysed the development of the pars basilaris occipitalis of 117 immature skeletons from the medieval necropolis at Mistihalj, in southern Yugoslavia. (6) Tocheri and Molto (2002) studied the pars basilaris, the maximum length of the femo-

ral diaphysis and the dental development. Their sample consisted of 39 skeletons from Kellis 2 (K2), a late Roman Period cemetery in Dakhleh, Egypt. (8)

Nagaoka et al. (2012) stated that the problem of these four studies is that most of them analysed undocumented specimens whose age was estimated from femoral diaphyseal length or body length. (9) (10) The studies did not have a statistical model for the estimation of age at death based on bone measurements. These circumstances are less fortunate than the background setting of this study, where the age of individuals was known to the day.

Nagaoka et al. (2012) studied the basilar part of the occipital bone of 272 Japanese fetuses between the third and eleventh month of gestational age. They also found that the dimensions of the occipital bones were positively correlated with the gestational ages and thereby confirmed previous results. However, the authors mentioned that there can exist differences in bone measurement regarding populations and that regression equations are population-related. The usefulness of regression equations in the determination of age at death based on the measurements of the bones was also confirmed in this study. (9) (10)

A frequent statement in forensic osteology is that when the width of the pars basilaris exceeds the maximum length, then the individual is aged five months postpartum. Figure 35 (p. 51) shows that this statement cannot be supported by the data and results of this study. Turner et al. (2013) came to the same conclusion when they found that the length can exceed the width at all ages. (67)

6.4 Conclusion and outlook

The current study reveals that skull measurements can be reliably used for the estimation of age at death in young children. Amongst these the height of the frontal bone as well as the oblique length of mandible are the most useful measurements for the aging of individuals.

The linear and quadratic regression equations introduced in this study can be meaningfully applied for the estimation of age at death by directly using skull bone measurements. Future studies should examine the relation between skull bone measurements and age at death of infants when considering the medical history, personal background as well as the characteristic of the populations under study. Thereby future research should concentrate on establishing valid and reproducible standards for skull-based aging methods, since these methods can be used in numerous bioarchaeological and forensic contexts.

References

1. Iscan MY. Age Markers in the Human Skeleton. Springfield, Illinois: Charles C. Thomas Publisher; 1989.
2. Baker B, Dupras T, Tocheri M. The Osteology of Infants and Children. Texas: Texas A & M University Press; 2005. 178 p.
3. Schour I, Massler M. The Development of the Human Dentition. J Am Dent Assoc. 1941;28:1153–60.
4. Scheuer L, Black S, Cunningham C. Developmental Juvenile Osteology. Academic Press; 2000. 600 p.
5. Fazekas IG, Kósa F. Forensic Fetal Osteology. Akadémiai Kiadó; 1978.
6. Redfield A. A new aid to aging immature skeletons: development of the occipital bone. Am J Phys Anthropol. 1970 Sep;33(2):207–20.
7. Scheuer L, MacLaughlin-Black S. Age estimation from the pars basilaris of the fetal and juvenile occipital bone. Int J Osteoarchaeol. 1994 Dec 1;4(4):377–80.
8. Tocheri MW, Molto JE. Aging fetal and juvenile skeletons from Roman Period Egypt using basiocciput osteometrics. Int J Osteoarchaeol. 2002 Sep 1;12(5):356–63.
9. Nagaoka T, Abe M, Shimatani K. Estimation of mortality profiles from non-adult human skeletons in Edo-period Japan. Anthropol Sci. 2012;120(2):115–28.
10. Nagaoka T, Kawakubo Y, Hirata K. Estimation of fetal age at death from the basilar part of the occipital bone. Int J Legal Med. 2012 May 30;126(5):703–11.
11. Cardoso HFV, Gomes J, Campanacho V, Marinho L. Age estimation of immature human skeletal remains using the post-natal development of the occipital bone. Int J Legal Med. 2013 Jan 11;127(5):997–1004.
12. Kósa F. Anthropological study for the determination of the Europid and Negroid characteristics on facial bones of human fetuses. Act Biol Szeged. 2002;46:83–90.
13. Malas MA, Üngör B, Tağıl SM, Sulak O. Determination of dimensions and angles of mandible in the fetal period. Surg Radiol Anat. 2006 Mar 28;28(4):364–71.
14. Minier M, Dedouit F, Maret D, Vergnault M, Mokrane F-Z, Rousseau H, et al. Fetal age estimation using MSCT scans of the mandible. Int J Legal Med. 2013 Nov 10;128(3):493–9.
15. Scheuer L. Application of osteology to forensic medicine. Clin Anat. 2002;15(4):297–312.

16. Scheuer JL, Musgrave JH, Evans SP. The estimation of late fetal and perinatal age from limb bone length by linear and logarithmic regression. *Ann Hum Biol.* 1980 Jan 1;7(3):257–65.
17. Sherwood RJ, Meindl R s., Robinson H b., May R I. Fetal age: Methods of estimation and effects of pathology. *Am J Phys Anthropol.* 2000 Nov 1;113(3):305–15.
18. Lewis ME, Gowland R. Brief and precarious lives: Infant mortality in contrasting sites from medieval and post-medieval England (AD 850–1859). *Am J Phys Anthropol.* 2007 Sep 1;134(1):117–29.
19. Miles AEW. The dentition in the assessment of individual age in skeletal material. In: Brothwell DR, editor. *Dental Anthropology*. Oxford: Pergamon Press; 1963.
20. Jordan RE, Kraus BS. *The Human Dentition Before Birth*. 1st ed. Philadelphia: Lea & Febiger; 1965. 218 p.
21. Reppien K, Sejrsen B, Lynnerup N. Evaluation of post-mortem estimated dental age versus real age: a retrospective 21-year survey. *Forensic Sci Int.* 2006 May 15;159 Suppl 1:S84–8.
22. Moorrees CFA, Fanning EA, Hunt EE. Age Variation of Formation Stages for Ten Permanent Teeth. *J Dent Res.* 1963 Nov 1;42(6):1490–502.
23. Demirjian A, Goldstein H, Tanner JM. A new system of dental age assessment. *Hum Biol.* 1973;45(2):211–27.
24. Ubelaker DH. *Human Skeletal Remains: Excavation, Analysis, Interpretation*. 2nd ed. Washington: Taraxacum; 1989.
25. Liversidge HM. Accuracy of age estimation from developing teeth of a population of known age (0–5.4 years). *Int J Osteoarchaeol.* 1994 Mar 1;4(1):37–45.
26. Manifold BM. Intrinsic and Extrinsic Factors Involved in the Preservation of Non-Adult Skeletal Remains in Archaeology and Forensic Science. *Forensic Sci Sem.* 2013;3(2):82–92.
27. Scheuer L, Black S. *The Juvenile Skeleton*. New York: Elsevier Academic Press; 2004.
28. Franklin D. Forensic age estimation in human skeletal remains: Current concepts and future directions. *Leg Med.* 2010 Jan;12(1):1–7.
29. Logan WHG, Kronfeld R. Development of the human jaws and surrounding structures from birth to the age of fifteen years. *J Am Dent Assoc.* 1933;20(3):379–427.
30. Kòsa F. Age estimation from the fetal skeleton. In: *Age markers in the human skeleton*. Springfield: Charles C. Thomas Publisher; 1989. p. 21–54.

31. Adalian P, Piercecchi-Marti MD, Bourliere-Najean B, Panuel M, Fredouille C, Dutour O, et al. Postmortem assessment of fetal diaphyseal femoral length: validation of a radiographic methodology. *J Forensic Sci.* 2001;46(2):215–9.
32. Saunders S, DeVito C, Herring A, Southern R, Hoppa R. Accuracy tests of tooth formation age estimations for human skeletal remains. *Am J Phys Anthropol.* 1993 Oct 1;92(2):173–88.
33. Black S, Scheuer L. Age Changes in the Clavicle: From the Early Neonatal Period to Skeletal Maturity. *Int J Osteoarchaeol.* 1996;6(5):425–34.
34. Castellana C, Kósa F. Estimation of fetal age from dimensions of atlas and axis ossification centers. *Forensic Sci Int.* 2001 Mar 1;117(1–2):31–43.
35. Castellana C, Kósa F. A multivariate method for classifying third to seventh cervical newborn vertebrae using bone measurements. *J Forensic Sci.* 2001 Nov;46(6):1434–7.
36. Kósa F, Castellana C. New forensic anthropological approachment for the age determination of human fetal skeletons on the base of morphometry of vertebral column. *Forensic Sci Int.* 2005 Jan 17;147, Supplement:S69–74.
37. Mărginean OM, Căpitănescu B, Mîndrilă I, Mărginean CM, Melinte PR. Study of the correlation between newborn and fetus ages and some morphometric cervical vertebral arches indices. *Romanian J Morphol Embryol Rev Roum Morphol Embryol.* 2008;49(3):387–90.
38. Leivhn WC. A cephalometric roentgenographic cross-sectional study of the craniofacial complex in fetuses from 12 weeks to birth. *Am J Orthod.* 1967 Nov;53(11):822–48.
39. A cephalometric appraisal of cranial and facial relationships at various stages of human fetal development: By Jorge C. Mestre, Jr., D.D.S., Eastman Dental Dispensary, Rochester, New York. *Am J Orthod.* 1959 Jan;45(1):62.
40. Manifold BM. Skeletal preservation of children's remains in the archaeological record. *HOMO - J Comp Hum Biol* [Internet]. 2015; Available from: <http://www.sciencedirect.com/science/article/pii/S0018442X15000748>
41. Byers SN. *Introduction to Forensic Anthropology*. Fourth Edition. Abingdon, Oxon: Routledge; 2010.
42. Parmar P, Rathod GB. DETERMINATION OF AGE BY STUDY OF SKULL SUTURES. *IJCRR* [Internet]. 2012;4(20). Available from: http://www.researchgate.net/profile/Dr_Prabhavathi_Paulraj/publication/232322829_MICROBIAL_DEGRADATION_OF_HYDROCARBONS_FROM_OIL_CONTAMINATED_SOIL_BY_USING_PSEUDOMONAS_SP/links/0f3175347b5d0913e6000000.pdf
43. Vijay Kumar A., Agarwal SS, G SM. Fusion of Skull Vault Sutures in Relation to Age: A Cross Sectional Postmortem Study Done in 3rd, 4th & 5th Decades of Life. *J Forensic R.* 2012 Mai;3(10).

44. White T, Folkens P. The Human Bone Manual. Amsterdam: Elsevier Ltd; 2005.
45. Krogman W. The problem of timing in facial growth, with special reference to period of the changing dentition. *Am J Orthod*. 1951;37(4):253–76.
46. Sperber GH. Craniofacial embryology. 4th ed. Wright Psg; 1989.
47. Anderhuber F, Pera F, Streicher J, Waldeyer A. Waldeyer Anatomie des Menschen. 19th ed. Berlin: De Gruyter; 2012.
48. Frazer EJ. The anatomy of the human skeleton. 2nd edition. J & A Churchill; 1920.
49. Aumüller G, Aust G, Doll A, Engele J, Kirsch J, Mense S, et al. Kopf. In: *Duale Reihe Anatomie*. 2. Auflage. Stuttgart: Thieme; 2007.
50. Braga J, Treil J. Estimation of pediatric skeletal age using geometric morphometrics and three-dimensional cranial size changes. *Int J Legal Med*. 2007 Nov;121(6):439–43.
51. Jain V, Suri SM, Jain A. Crown-Rump Length estimation of Human Fetuses by external surface area of Right Parietal bone. *IAIM*. 2015;2(2):77–83.
52. Watson E, Lowrey G. Growth and Development of children. Year Book Medical Publishers; 1962.
53. Dauber W. Feneis' Bild-Lexikon der Anatomie. 9. Auflage. Stuttgart: Thieme; 2005.
54. Stiebitz R. Die Schädelammlung des Valentin Terzer. *Österr Zahnärzte Ztg*. 1997;(6):32–4.
55. Pawlowsky V. Mutter ledig, Vater Staat: das Gebär- und Findelhaus in Wien 1784-1910. Innsbruck: Studien Verlag; 2001.
56. Schaefer M, Black S, Scheuer L. Chapter 1 - The Head and Neck. In: Scheuer MSB, editor. *Juvenile Osteology*. San Diego: Academic Press; 2009. p. 1–66.
57. R Core Team. R: A Language and Environment for Statistical Computing [Internet]. Version 3.0.1. R Foundation for Statistical Computing, editor. Vienna, Austria.; 2013. Available from: <http://www.R-project.org/>
58. Wickham H. *ggplot2: elegant graphics for data analysis*. New York: Springer; 2009.
59. Molinaro AM, Simon R, Pfeiffer RM. Prediction error estimation: a comparison of resampling methods. *Bioinformatics*. 2005;21(15):3301–7.
60. Hanneman RA, Kposowa AJ, Riddle MD. *Basic Statistics for Social Research*. 1 edition. San Francisco, CA: Jossey-Bass; 2012. 560 p.

61. Jukic AM, Baird DD, Weinberg CR, McConaughy DR, Wilcox AJ. Length of human pregnancy and contributors to its natural variation. *Hum Reprod Oxf Engl.* 2013 Oct;28(10):2848–55.
62. Bassed RB, Briggs C, Drummer OH. The incidence of asymmetrical left/right skeletal and dental development in an Australian population and the effect of this on forensic age estimations. *Int J Legal Med.* 2012 Mar;126(2):251–7.
63. Rissech C, Wilson J, Winburn AP, Turbón D, Steadman D. A comparison of three established age estimation methods on an adult Spanish sample. *Int J Legal Med.* 2012 Jan;126(1):145–55.
64. Pawlowsky V. Das “Aussetzen überlästiger und nachtheiliger Kinder” Die Wiener Findelanstalt 1784-1910. *Österreichische Zeitschrift für Geschichtswissenschaften.* 2014;25(1+2):18–40.
65. Muskaan A, Sarkar S. Mandible-An Indicator for age and sex determination using digital Orthopantomogram. *Sch J Dent Sci.* 2015;2(1):82–95.
66. Bareggi R, Sandrucci MA, Baldini G, Grill V, Zweyer M, Narducci P. Mandibular growth rates in human fetal development. *Arch Oral Biol.* 1995 Feb;40(2):119–25.
67. Turner C, Burrell C, Carpenter R, Ohman J. Biological age estimation of subadult human skeletal remains: Comparison of dental development with the humerus, femur and pars basilaris [Internet]. Poster presented at; 2013 [cited 2015 Sep 21]. Available from: http://www.academia.edu/7349616/Biological_age_estimation_of_subadult_human_skeletal_remains_Comparison_of_dental_development_with_the_humerus_femur_and_pars_basilaris

List of Figures

Figure 1: Anterior view of the fetal skull. (4)	15
Figure 2: Lateral view of the fetal skull. (4)	15
Figure 3: Basal view of the fetal skull. (4)	16
Figure 4: Basilar and lateral parts of the occipital bone at the age of 3 - 10 lunar months. (5)	20
Figure 5: Intracranial view of the perinatal occipital bone. (27)	21
Figure 6: The right perinatal parietal bone. (27).....	22
Figure 7: Perinatal frontal and parietal bones. (27)	23
Figure 8: Lateral view of the right perinatal zygomatic bone. (27).....	24
Figure 9: Palatal view of the right maxilla. (27)	25
Figure 10: Frontal view of a child's mandible at the dental age of one year. (27).....	26
Figure 11: Foundling house in Vienna (Alserstrasse 23) in the first decade of the 20 th century. (55) ...	29
Figure 12: Transfer of children from the biological mothers to the midwives and the foster mothers. (55)	29
Figure 13: The analysed individuals of the Terzer collection Part I.	31
Figure 14: The analysed individuals of the Terzer collection Part II.	32
Figure 15: The height of the occipital squama.	35
Figure 16: The width of the occipital squama.	35
Figure 17: The maximum width of the pars basilaris occipitalis.	36
Figure 18: The sagittal length of the pars basilaris occipitalis.	36
Figure 19: The maximum length of the pars basilaris occipitalis.	37
Figure 20: The height of the parietal bone.	37
Figure 21: The width of the parietal bone.	38
Figure 22: The height of the frontal bone.	38
Figure 23: The width of the frontal bone.	39
Figure 24: The length of the zygomatic bone.	39
Figure 25: The width (oblique height) of the zygomatic bone.	40
Figure 26: The length of the maxilla.	40
Figure 27: The body length of the mandible.	41
Figure 28: The width of the mandible.	41
Figure 29: The full length of the half mandible (oblique length).....	42
Figure 30: Linear and quadratic regressions of the chord height of the pars squama occipitalis.....	46
Figure 31: Linear and quadratic regressions of the chord width of the pars squama occipitalis.	47
Figure 32: Linear and quadratic regressions of the maximum width of the pars basilaris occipitalis. ...	48
Figure 33: Linear and quadratic regressions of the sagittal length of the pars basilaris occipitalis.....	49
Figure 34: Linear and quadratic regressions of the maximum length of the pars basilaris occipitalis. ..	50

Figure 35: Relationship between the maximum width and the maximum length of the pars basilaris...	51
Figure 36: Linear and quadratic regressions of the chord height of the parietal bone.	52
Figure 37: Linear and quadratic regressions of the chord width of the parietal bone.	53
Figure 38: Linear and quadratic regressions of the chord height of the frontal bone.	54
Figure 39: Linear and quadratic regressions of the chord width of the frontal bone.	55
Figure 40: Linear and quadratic regressions of the length of the zygomatic bone.	56
Figure 41: Linear and quadratic regressions of the oblique height (width) of the zygomatic bone.	57
Figure 42: Linear and quadratic regressions of the length of the maxilla.....	58
Figure 43: Linear and quadratic regressions of the body length of the mandible.	59
Figure 44: Linear and quadratic regressions of the width of the mandible.	60
Figure 45: Linear and quadratic regressions of the oblique length of the mandible.	61

List of Tables

Table 1: Individuals of the Terzer collection with information about age at death and cause of death..	33
Table 2: Summary of all measurements taken.....	34
Table 3: Descriptive statistics of the measurements.....	45
Table 4: Model assessment for the chord height of the pars squama occipitalis.....	46
Table 5: Model assessment for the chord width of the pars squama occipitalis.	47
Table 6: Model assessment and comparison with Scheuer & MacLaughlin-Black, 1994, for the maximum width of the pars basilaris occipitalis.	48
Table 7: Model assessment and comparison with Scheuer & MacLaughlin-Black, 1994, for the sagittal length of the pars basilaris occipitalis.	49
Table 8: Model assessment and comparison with Scheuer & MacLaughlin-Black, 1994, for the maximum length of the pars basilaris occipitalis.....	50
Table 9: Model assessment for the chord height of the parietal bone.....	52
Table 10: Model assessment for the chord width of the parietal bone.	53
Table 11: Model assessment for the chord height of the frontal bone.....	54
Table 12: Model assessment for the chord width of the frontal bone	55
Table 13: Model assessment for the length of the zygomatic bone.....	56
Table 14: Model assessment for the oblique height (width) of the zygomatic bone.	57
Table 15: Model assessment for the length of the maxilla.	58
Table 16: Model assessment for the body length of the mandible.....	59
Table 17: Model assessment for the width of the mandible.	60
Table 18: Model assessment for the oblique length of the mandible.....	61
Table 19: Measurements sorted by the value of R^2 of linear and quadratic regression.	62

Abbreviations

SD Standard deviation

S.E.E. Standard Error of Estimate

M.A.D. Mean Absolute Deviation

CV error Leave-one-out-cross-validation

R^2 Adjusted R-squared (= coefficient of determination)

Min. Minimum

Max. Maximum

Supplemental Material

Number of the Individuum	Age (months/years)	Age (days)		The Occipital	
				1 Chord height pars squama occipitalis	2 Chord width pars squama occipitalis
P210_ZE-000300	7 months	213	300	48,9	47,1
P210_ZE-000301	2 months, 28 days	89	301	55,6	56,9
P210_ZE-000302	3 months, 9 days	100	302	51,4	56,4
P210_ZE-000303	3 months, 15 days	106	303	57,8	62,6
P210_ZE-000304	3 months, 20 days	111	304	68,8	68,3
P210_ZE-000305	4 months, 5 days	127	305	62	59,5
P210_ZE-000306	9 months, 15 days	289	306	65,4	60,4
P210_ZE-000308	7 months, 13 days	226	308	66,7	75,9
P210_ZE-000310	4 months, 12 days	134	310	67,9	68,7
P210_ZE-000311	6 months, 28 days	211	311	74,1	69,6
P210_ZE-000312	10 months, 17 days	321	312	67,5	67,9
P210_ZE-000314	1 year, 17 days	382	314	73,4	85,9
P210_ZE-000316	1 year, 4 months, 14 days	501	316	74,7	88,6
P210_ZE-000317	1 year, 5 months, 27 days	544	317	70,4	71,4
P210_ZE-000318	9 months, 12 days	286	318	87,3	85,4
P210_ZE-000319	1 year, 9 months	639	319	84,7	85,1
P210_ZE-000320	6 months, 15 days	198	320	63	66,1
P210_ZE-000321	5 months, 1 day	153	321	63,7	65,1
P210_ZE-000322	1 month, 1 day	31	322	56,4	57,2
P210_ZE-000323	8 months, 2 days	245	323	63	68,7
P210_ZE-000324	17 days	11	324	52,2	52,6
P210_ZE-000326	4 days	4	326	51,9	59,7
P210_ZE-000328	2 months, 14 days	75	328	54,9	56,7
P210_ZE-000329	8 months, 26 days	178	329	56,6	62,9
P210_ZE-000331	10 months, 1 day	305	331	73,8	77,1
P210_ZE-000332	1 year, 6 months	548	332	-	-
P210_ZE-000333	1 year, 4 months	487	333	-	-
P210_ZE-000334	1 year, 9 months, 8 days	647	334	77,1	80,8
P210_ZE-000335	1 year, 10 months, 10 days	679	335	85,3	92,9
P210_ZE-000336	1 year, 11 months	700	336	88,2	88,6
P210_ZE-000337	2 years, 7 months, 22 days	965	337	83,5	91,5
P210_ZE-000338	1 year, 8 months	608	338	-	-

	The Occipital				The Parietal			The Frontal	
	1 Maximum width basilaris	2 Sagittal length basilaris	3 Maximum length basilaris		1 Chord height	2 Chord width		1 Chord height	2 Chord width
300	8,1	8,3	11,2	300	60,1	62,7	300	45,1	34,8
301	12,6	9,9	12,5	301	68,4	73	301	47,6	43,5
302	9,5	8,8	11,9	302	63,2	66,9	302	46,4	42,5
303	12,5	10,3	14,4	303	75,2	81,3	303	53,3	43,5
304	14,3	10,6	14	304	91,6	83,8	304	59,9	52,4
305	13,9	10,5	14,4	305	74	78,8	305	54,3	49,3
306	12,5	10,4	14,8	306	84,7	85,6	306	56,5	51
308	13,5	12,2	14,1	308	83,4	89,2	308	61,9	53,2
310	13,6	11,9	16,3	310	82,4	78,4	310	60,7	48,8
311	14,1	10	14,4	311	75,6	86,8	311	57,3	49,9
312	15,3	10,3	15,6	312	78,8	83,1	312	57,5	51,1
314	14,1	11,4	15,6	314	89,2	93,2	314	63,9	57
316	20	15,1	19,5	316	98,1	94,6	316	72,5	60,2
317	15,5	10,8	14,8	317	83,6	86,1	317	59,1	50,5
318	14,6	12,1	15,6	318	89,9	117	318	67	56,2
319	17,2	12,5	17,5	319	93,9	101,3	319	69,7	61,2
320	15,6	11,9	16,5	320	78,2	85,3	320	52,4	48,5
321	14,1	11,1	16,1	321	76,4	78,4	321	53,5	49,8
322	10,4	9,3	12,8	322	63,6	67,5	322	45,5	40,3
323	13,1	11,3	15,1	323	82,1	75,6	323	56,4	48,4
324	13,2	13,8	15,5	324	66,8	72,2	324	50,1	46,6
326	14,3	13,7	17,2	326	73,5	80,3	326	53,5	49,8
328	11,9	9,7	12,2	328	73,7	76,2	328	48,3	47,1
329	12,9	11,6	14,2	329	83,1	84,2	329	53,8	54
331	15,5	12,9	16,5	331	85,8	94,1	331	59,6	58
332	16,9	12	17,1	332	-	-	332	-	-
333	17,2	12,3	18,8	333	-	-	333	-	-
334	12,4	11,1	15,2	334	92,4	89,6	334	69,4	60,2
335	16,9	13,7	17	335	98,5	106,8	335	71,1	58,4
336	15,1	13,9	17,5	336	101,4	109,7	336	74	68,3
337	24,2	16,6	23,2	337	96,6	111,5	337	85,9	-
338	18,5	14,3	20,1	338	-	-	338	-	-

	The Zygomatic		The Maxilla			The Mandible		
	1 Length	2 Oblique height (Width)		1 Length		1 Body length	2 Width	3 Oblique length
300	19,7	14,2	300	21,6	300	29,1	10,4	37,5
301	23,6	20,3	301	26,7	301	35,3	16,1	51,4
302	25,9	19,5	302	26	302	34,6	16	48,1
303	23,2	18,3	303	24,6	303	34,1	14,9	49,2
304	31,5	23,3	304	26,1	304	39,5	18,9	56,6
305	26,9	21,3	305	28,3	305	38	16,2	53,9
306	24,6	19,7	306	27	306	38,9	12,5	52,5
308	25,3	19,8	308	25,5	308	39,7	15,1	59,1
310	22,9	17,6	310	28,8	310	38,1	15,2	57,1
311	27,5	19,7	311	27,9	311	40,3	16,6	56,9
312	27,4	19,9	312	27,9	312	39	14,9	54,1
314	27,3	21,5	314	32,2	314	41,4	-	60,6
316	-	-	316	34,2	316	50,2	-	-
317	28,9	22,4	317	28,2	317	39,5	15,9	53,9
318	30,3	22,7	318	29,7	318	46,5	17,2	65,5
319	27,5	23,3	319	29	319	43,7	16,9	64,8
320	28,6	21,2	320	30	320	40,2	17,5	55,7
321	25,9	20,2	321	29,1	321	36,5	14,8	52,6
322	25,3	17,4	322	25,9	322	31,7	11,2	44,9
323	26,5	23,8	323	26,8	323	38,3	12,4	55
324	17	14,3	324	25,2	324	32,3	17,1	43,2
326	17,6	18,3	326	28,8	326	38,9	17,7	53,6
328	24,1	18,4	328	26,7	328	35,3	12,7	51,6
329	25,6	18,4	329	-	329	34,4	15,3	53,1
331	31,7	23,6	331	28,7	331	46	16,5	66
332	35,5	24,6	332	30,7	332	46,3	17,7	68,9
333	32,1	25,3	333	30,8	333	45,3	16,9	71,2
334	30,7	23,1	334	28,1	334	40,4	14,2	58,6
335	32,8	27,9	335	32,8	335	49,4	18,9	74,5
336	39,5	26,7	336	34,4	336	43,7	19,3	71,7
337	-	-	337	37	337	57,2	24,5	82,7
338	30,5	26,9	338	30	338	49,5	20,4	75,1

Curriculum Vitae

Personal data

Name: Sandra Reithmayer

Date of birth: 11th February 1987

Place of birth: Vienna, Austria

Nationality: Austrian

Email: sandra.reithmayer@gmail.com

Education

2013 - 2015 Study of Anthropology, University of Vienna

2005 - 2013 Study of Biology, University of Vienna

1997 - 2005 Gymnasium Albertus Magnus Schule der Marianisten, Vienna

1993 - 1997 Volksschule Albertus Magnus Schule der Marianisten, Vienna